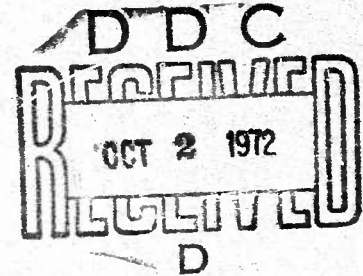


AD 749256

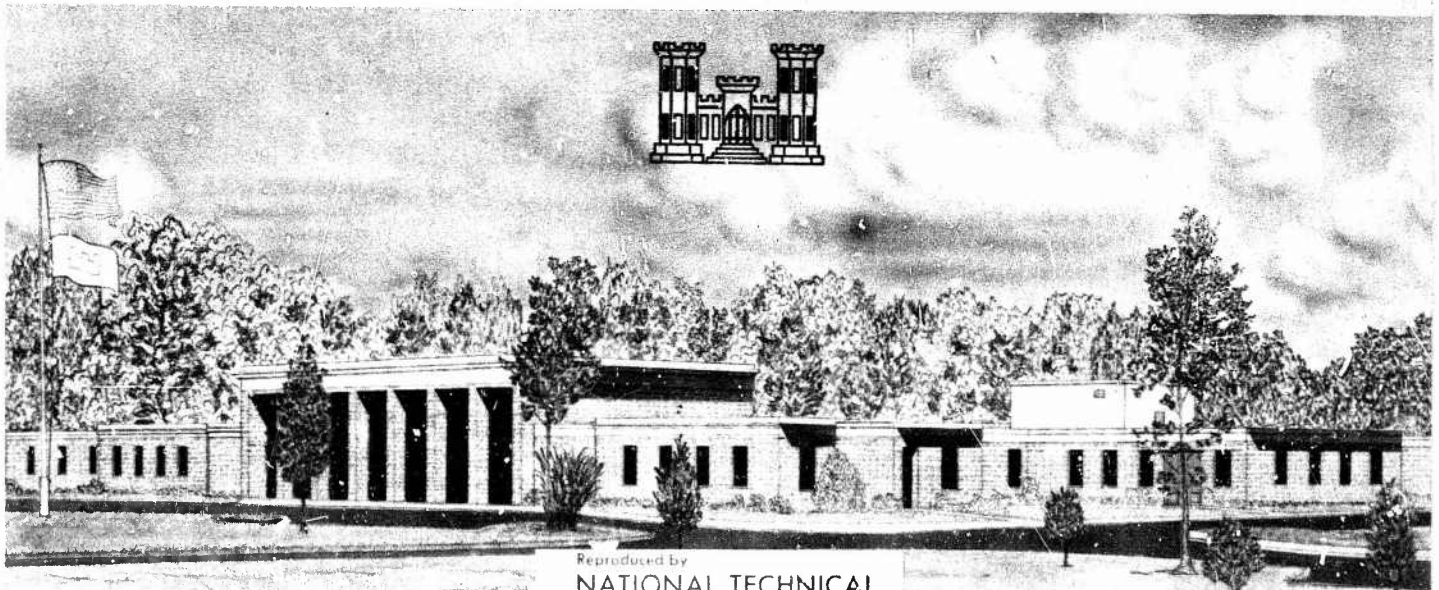


MISCELLANEOUS PAPER S-72-35

HYDROSTATIC AND SHEAR RESPONSES OF TWO TUFF MATERIALS UNDER VARIOUS RATES OF STRESS

by

J. Q. Ehrgott



Reproduced by
NATIONAL TECHNICAL
INFORMATION SERVICE
U S Department of Commerce
Springfield VA 22151

September 1972

Sponsored by Defense Nuclear Agency

Conducted by U. S. Army Engineer Waterways Experiment Station
Soils and Pavements Laboratory
Vicksburg, Mississippi

APPROVED FOR PUBLIC RELEASE; DISTRIBUTION UNLIMITED

15-5

Unclassified

Security Classification

DOCUMENT CONTROL DATA - R & D

(Security classification of title, body of abstract and indexing annotation must be entered when the overall report is classified)

1. ORIGINATING ACTIVITY (Corporate author) U. S. Army Engineer Waterways Experiment Station Vicksburg, Mississippi		2a. REPORT SECURITY CLASSIFICATION Unclassified	
		2b. GROUP	
3. REPORT TITLE HYDROSTATIC AND SHEAR RESPONSES OF TWO TUFF MATERIALS UNDER VARIOUS RATES OF STRESS			
4. DESCRIPTIVE NOTES (Type of report and inclusive dates) Final report			
5. AUTHOR(S) (First name, middle initial, last name) John Q. Ehrgott			
8. REPORT DATE September 1972		7a. TOTAL NO. OF PAGES 64	7b. NO. OF REFS 2
8a. CONTRACT OR GRANT NO.		9a. ORIGINATOR'S REPORT NUMBER(S) Miscellaneous Paper S-72-35	
b. PROJECT NO.			
c.		9b. OTHER REPORT NO(S) (Any other numbers that may be assigned this report)	
d.			
10. DISTRIBUTION STATEMENT Approved for public release; distribution unlimited			
11. SUPPLEMENTARY NOTES		12. SPONSORING MILITARY ACTIVITY Defense Nuclear Agency Washington, D. C.	
13. ABSTRACT <p>A limited laboratory testing program was conducted on materials cored from two tunnels at the Nevada Test Site, Mercury, Nevada. The materials were grouped into three different tuffs. The purposes of the study were to investigate the loading-rate effects and the response characteristics of the materials from the two tunnels. Both static (rise time of approximately 1 minute) and dynamic (rise time of 2 to 50 msec) hydrostatic and triaxial shear tests were conducted in the U. S. Army Engineer Waterways Experiment Station's new dynamic high-pressure triaxial test device. Although the test program was very limited, the test data do provide some insight into the hydrostatic and shear response of the tuff materials tested. The test data indicate some of the material did exhibit loading-rate effects and there were differences in the response characteristics of the specimens from the two tunnels as well as differences in the response characteristics of different specimens from one of the tunnels.</p>			

DD FORM 1473
1 NOV 65REPLACES DD FORM 1473, 1 JAN 64, WHICH IS
OBSOLETE FOR ARMY USE.Unclassified
Security Classification

14.	KEY WORDS	LINK A		LINK B		LINK C	
		ROLE	WT	ROLE	WT	ROLE	WT
	Hydrostatic tests Rock test specimens Triaxial shear tests Tuff Tunnels						

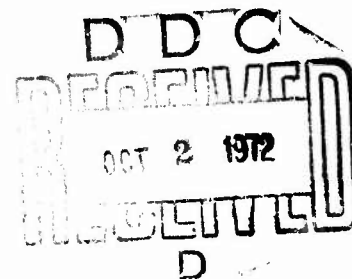


MISCELLANEOUS PAPER S-72-35

HYDROSTATIC AND SHEAR RESPONSES OF TWO TUFF MATERIALS UNDER VARIOUS RATES OF STRESS

by

J. Q. Ehrgott



September 1972

Sponsored by Defense Nuclear Agency

Conducted by U. S. Army Engineer Waterways Experiment Station
Soils and Pavements Laboratory
Vicksburg, Mississippi

ARMY-MRC VICKSBURG, MISS

APPROVED FOR PUBLIC RELEASE; DISTRIBUTION UNLIMITED

THE CONTENTS OF THIS REPORT ARE NOT TO BE
USED FOR ADVERTISING, PUBLICATION, OR
PROMOTIONAL PURPOSES. CITATION OF TRADE
NAMES DOES NOT CONSTITUTE AN OFFICIAL EN-
DORSEMENT OR APPROVAL OF THE USE OF SUCH
COMMERCIAL PRODUCTS.

ABSTRACT

A limited laboratory testing program was conducted on materials cored from two tunnels at the Nevada Test Site, Mercury, Nevada. The materials were grouped into three different tuffs. The purposes of the study were to investigate the loading-rate effects and the response characteristics of the materials from the two tunnels.

Both static (rise time of approximately 1 minute) and dynamic (rise time of 2 to 50 msec) hydrostatic and triaxial shear tests were conducted in the U. S. Army Engineer Waterways Experiment Station's new dynamic high-pressure triaxial test device. Although the test program was very limited, the test data do provide some insight into the hydrostatic and shear response of the tuff materials tested. The test data indicate some of the material did exhibit loading-rate effects and there were differences in the response characteristics of the specimens from the two tunnels as well as differences in the response characteristics of different specimens from one of the tunnels.

PREFACE

The investigation described in this report was conducted by personnel of the U. S. Army Engineer Waterways Experiment Station (WES) and was funded by the Test Command, Defense Nuclear Agency. The project officer was Dr. B. Grote of Test Command. Terra Tek, Inc. (TT), provided the precut tuff cores used in the investigation. Mr. Sidney Green of TT provided helpful comments and advice during the course of study.

The investigation was conducted by personnel of the Soils and Pavement Laboratory, WES, and the report was prepared by Mr. J. Q. Ehrgott, Impulse Loads Section (ILS), Soil Dynamics Branch, Soils and Pavement Laboratory. Mr. R. L. Stowe, Engineering Mechanics Branch, Concrete Laboratory, conducted the Brazilian tensile tests. Mr. P. F. Hadala, ILS, provided guidance in the analysis of the data. Dr. J. G. Jackson, Jr., was Chief of ILS, Mr. R. W. Cunny was Chief of the Soil Dynamics Branch, and Mr. J. P. Sale was Chief of the Soils and Pavement Laboratory. Director of WES was COL Ernest D. Peixotto, CE, and the Technical Director was Mr. F. R. Brown.

CONTENTS

ABSTRACT-----	4
PREFACE-----	5
CONVERSION FACTORS, BRITISH TO METRIC UNITS OF MEASUREMENT-----	8
CHAPTER 1 INTRODUCTION-----	9
1.1 Background-----	9
1.2 Purpose-----	9
1.3 Scope-----	10
CHAPTER 2 TEST EQUIPMENT, SPECIMENS, AND PROCEDURES-----	11
2.1 Dynamic High-Pressure Triaxial Test Device-----	11
2.2 Hydrostatic and Shear Tests-----	11
2.3 Material Received by WES-----	12
2.4 Procedure for Handling the Tuff-----	13
CHAPTER 3 MATERIAL DESCRIPTIONS AND SPECIAL TESTS-----	15
3.1 Tunnel U12e-12 Tuff-----	15
3.2 Tunnel U12n-06 Tuff-----	16
3.3 Special Tests on U12e-12 Tuff-----	16
3.4 Special Tests on U12n-06 Tuff-----	17
3.5 Comparison Between U12e-12 and U12n-06 Tuff-----	17
CHAPTER 4 CONSTITUTIVE PROPERTY TESTS ON TUNNEL U12e-12 TUFF-----	23
4.1 Hydrostatic Tests-----	23
4.2 Shear Tests-----	25
CHAPTER 5 CONSTITUTIVE PROPERTY TESTS ON U12n-06 TUFF-----	37
5.1 Hydrostatic Tests-----	37
5.2 Shear Tests-----	38
CHAPTER 6 COMPARISON OF THE TUFF MATERIALS-----	47
6.1 Hydrostatic Response-----	47
6.2 Shear Response-----	48
CHAPTER 7 SUMMARY-----	52
7.1 U12e-12 Tuff-----	52
7.2 U12n-06 Tuff-----	52
7.3 Differences Noted Between Tuffs-----	52
TABLES	
3.1 Composition Properties of Tunnel U12e-12 Tuff-----	19
3.2 Composition Properties of Tunnel U12n-06 Tuff-----	20
FIGURES	
3.1 Specimen weight versus time for five pieces of tuff placed in three different environments-----	21

FIGURES

3.2	Dry unit weight versus water content for tuff from Tunnels U12e-12 and U12n-06-----	22
3.3	Brazilian tensile tests-----	22
4.1	Stress-strain data from hydrostatic tests conducted on tuff from Tunnel U12e-12, Boring 7B-----	27
4.2	Stress-strain data from hydrostatic tests conducted on tuff from Tunnel U12e-12, Site B-----	28
4.3	Stress versus volumetric strain showing the hydrostatic response of tuff from Tunnel U12e-12-----	29
4.4	Shear test results from Test E12.7B.8.0 showing axial and radial strain response-----	30
4.5	Shear test results from Test E12.7B.8.6 showing axial and radial strain response-----	31
4.6	Shear test results from Test E12.7B.10.2 showing axial and radial strain response-----	32
4.7	Shear test results from Test E12.SB.9.6 showing axial and radial strain response-----	33
4.8	Shear test results from Test E12.SB.16.5 showing axial and radial strain response-----	34
4.9	Principal stress difference versus principal strain dif- ference showing results from shear tests conducted on tuff from Tunnel U12e-12-----	35
4.10	Principal stress difference versus mean normal stress showing peak stresses from five shear tests on tuff from Tunnel U12e-12-----	36
5.1	Stress-strain data from hydrostatic tests conducted on tuff from Tunnel U12n-06, Boring DB2-----	40
5.2	Stress versus volumetric strain showing the hydrostatic response of tuff from Tunnel U12n-06-----	41
5.3	Shear test results from Test N06.2.26.7 showing axial and radial strain response-----	42
5.4	Shear test results from Test N06.2.27.C showing axial and radial strain response-----	43
5.5	Shear test results from Test N06.2.31.0 showing axial and radial strain response-----	44
5.6	Principal stress difference versus principal strain dif- ference showing results of shear tests on tuff from Tunnel U12n-06-----	45
5.7	Principal stress difference versus mean normal stress showing peak stresses from shear tests on tuff from Tunnel U12n-06-----	46
6.1	Stress versus volumetric strain showing the average hydrostatic responses for the tuff tested-----	49
6.2	Principal stress difference versus principal strain dif- ference showing average shear responses for the tuff tested-----	50
6.3	Principal stress difference versus mean normal stress showing the peak stress from the shear tests conducted on tuff from Tunnels U12e-12 and U12n-06-----	51

CONVERSION FACTORS, BRITISH TO METRIC UNITS OF MEASUREMENT

British units of measurement used in this report can be converted to metric units as follows:

<u>Multiply</u>	<u>By</u>	<u>To Obtain</u>
mils	0.0254	millimeters
inches	2.54	centimeters
feet	0.3048	meters
pounds (force) per square inch	0.6894757	newtons per square centimeter

CHAPTER 1

INTRODUCTION

1.1 BACKGROUND

The U. S. Army Engineer Waterways Experiment Station (WES) was requested by the Test Command, Defense Nuclear Agency (DNA), to participate in a program involving two high-explosive (HE) events conducted in Tunnels U12e-12 and U12n-06 within Rainier Mesa, Nevada Test Site (NTS), Mercury, Nevada. The program was an outgrowth of the need for a better understanding of how the rocks surrounding a tunnel behave when subjected to shock from an underground nuclear test upon execution within a horizontal-line-of-sight (HLOS) configuration. The ultimate purpose of the program, in conjunction with other studies, is to insure competence in containment operations so as to preclude exposures of HLOS experiments to unacceptable environments and to prevent the release of radioactive substance into the atmosphere. Other agencies participating in these tests included Terra Tek, Inc. (TT), Stanford Research Institute (SRI), and Systems, Science, and Software (S³).

Static laboratory testing to determine the material properties of the tuff materials obtained from the two tunnels was performed by TT. WES was requested to conduct a series of dynamic hydrostatic and tri-axial shear tests with loading times to peak stress of 2 to 50 msec on selected specimens of tuff provided by TT. These specimens were thought to be representative of each of the two HE test locations, i.e. Tunnels U12e-12 and U12n-06.

1.2 PURPOSE

The purpose of the WES test program was to investigate the loading-rate effects and response characteristics of the rocks that form the walls of the two tunnels that have been used for nuclear tests. Differences in the response characteristics of the two materials were to be noted.

1.3 SCOPE

This report documents the results of a series of dynamic (2- to 50-msec loading time to peak stress) and static (1-minute loading time to peak stress) hydrostatic and triaxial shear tests conducted on the tuff materials from Tunnels U12e-12 and U12n-06. The tests on the U12e-12 tuff consisted of two static hydrostatic and triaxial shear tests, three dynamic hydrostatic and triaxial shear tests, and one dynamic hydrostatic loading test. The tests on U12n-06 tuff consisted of one static hydrostatic and triaxial shear test, two dynamic hydrostatic and triaxial shear tests, and one dynamic hydrostatic loading and unloading test. Stress levels as high as 8,000 psi¹ were applied to permit correlation with TT data from tests to be conducted at approximately the same pressure level.

¹ A table of factors for converting British units of measurement to metric units is presented on page 8.

CHAPTER 2

TEST EQUIPMENT, SPECIMENS, AND PROCEDURES

2.1 DYNAMIC HIGH-PRESSURE TRIAXIAL TEST DEVICE

The laboratory testing program consisted of both hydrostatic and shear tests conducted in the WES dynamic, high-pressure triaxial test device (DHT).² In general, the DHT is used to develop controlled dynamic pressure pulses in the fluid-filled triaxial chamber. Dynamic axial pulse loads are developed by a pneumatic ram loader (SECO) that is time synchronized with the DHT. Together the DHT and SECO can be operated in a testing program so as to provide time varying confining pressures and axial loads on cylindrically shaped, membrane-covered test specimens contained within the oil-filled triaxial chamber.

Time histories of the applied axial load, the chamber pressure loading, and the specimen deformation response to those loadings are measured within the triaxial test chamber. The measurements that are recorded as a function of time throughout the test are chamber pressure, axial load delivered to the specimen, axial piston travel, vertical deformation of the specimen, and specimen diameter change. Vertical deformation is measured by two linear variable differential transformer (LVDT) units that monitor specimen top-cap movement. Three LVDT units, mounted in a horizontal plane at 120-degree intervals around the specimen at its midheight, measure lateral deformations.

2.2 HYDROSTATIC AND SHEAR TESTS

In the hydrostatic tests, the specimens were loaded by the same pressure in all directions. Measurements of pressure, axial deformation, and lateral deformation were used to calculate mean normal pressure p , axial strain ϵ_a , radial strain ϵ_r , and volumetric strain

² J. C. Ehrgott; "Development of a Dynamic High-Pressure Triaxial Test Device"; in preparation; U. S. Army Engineer Waterways Experiment Station, CE, Vicksburg, Mississippi.

$\Delta V/V_0$. The calculations of strains were based on original specimen height and diameter. Volumetric strain was taken as the sum of

$$\epsilon_a + 2\epsilon_r.$$

The shear test was conducted after the hydrostatic test. Once the peak hydrostatic pressure was reached, it was held constant. The specimen was then loaded in the axial direction until the specimen could no longer support additional load. In several tests, the confining pressure was also increased as the axial load was increased so as to provide information on specimen response under a constant stress ratio loading path.

Measurements made during the shear tests included chamber pressure, applied axial load, and axial and lateral deformation. These data were used to calculate the radial stress σ_r , the deviator load, and the axial and radial strains. Principal stress difference $\sigma_a - \sigma_r$ was calculated from the deviator load and the current specimen cross-sectional area. It should be noted that the axial direction of the specimen in this testing program was taken along the axis of core as received from TT and is the axial direction of the drill hole from which the core was obtained in the field.

2.3 MATERIAL RECEIVED BY WES

The tuff material was received from TT in two shipments. The first shipment was received on 27 May 1971 and included five cylindrical, NX-size-diameter cores of the U12e-12 tuff material. At the request of WES, TT had precut the cores to 5-inch lengths. Each core was wrapped in foil and waxed; the ends of each core were covered by a piece of moist cloth and sealed with a piece of plastic wrap. Each core was contained in a sealed plastic bag. The second shipment was received on 9 July 1971 and included seven U12e-12 cores and five U12n-06 cores. The U12e-12 cores in the shipment were not from the same borings as those in the earlier shipment and were designated on the identification tags as being from Site B. The cores in this shipment were also NX size and precut by TT to 5-inch lengths. These cores were also sealed in individual plastic bags. Each core was wrapped in foil and waxed, but the

ends were not covered. All the cores from both shipments were stored in the as-received condition in a controlled-humidity room (humid room) with relative humidity between 95 and 100 percent.

2.4 PROCEDURE FOR HANDLING THE TUFF

Prior to testing, each specimen was assigned a three-part identification number that was coded to identify tunnel, boring, and location (distance drilled into tunnel wall). For example, Specimen E12.7B.8.6 came from Tunnel U12e-12, Boring DB7B, 8.6 to 9.1 feet into the tunnel wall.

For testing, each specimen was removed from the humid room, the time noted, and the plastic bag and wrappings removed. The specimen was weighed, and measurements of the height and diameter were taken. A description of the specimen was noted. The specimen was placed on the steel base pedestal of the triaxial test device, and a rubber triaxial-specimen membrane was placed over the specimen. The membrane was sealed to the pedestal and to a steel top cap by the use of rubber bands. The time was noted. The average time of specimen exposure was approximately 10 minutes. A thin coat of a liquid rubber compound, Gage Coat 2, was painted on the membrane to prevent deterioration of the rubber membrane in the oil-filled triaxial chamber. The measurement units of the triaxial test device were assembled, and the specimen was placed in the triaxial test chamber. It should be noted that the ends of the cores were not lapped, since it was felt that the lapping procedure would allow the specimens to lose additional water. Thus, all cores were tested with sawed ends, the condition in which they were received at WES.

Following the loading test, the specimen was removed from the device, and the time was noted. The rubber membrane was stripped from the specimen, and the specimen was weighed. The time was again noted. The average time for this procedure was 5 minutes. The specimen surface was inspected for oil to determine if the membrane had broken during the test. The final height and diameter measurements were made, and a photograph of the specimen was taken. The specimen was then placed in an

oven at 106-110 C. When the specimen showed no further weight loss, which was generally after two to three days, the dry weight was recorded.

The volume of the specimen was calculated from the first set of measurements obtained on the specimen. The as-received water content w (ratio of weight of water to weight of dry material) and as-received wet unit weight γ (ratio of total specimen weight to specimen volume) were calculated based on the pretest weight of the specimen. The exposed water content and exposed wet unit weight were calculated based on the posttest specimen weight. The largest differences noted between the as-received and exposed wet unit weights and water contents were $\Delta\gamma = 0.01 \text{ g/cm}^3$ and $\Delta w = 0.6$ percent, respectively.

Several of the specimens were received in a broken condition and could not be tested. However, water content and wet unit weight measurements were made on the broken specimens. The volume of each of these broken pieces was determined by a mercury-displacement technique. In addition, several of the broken pieces of core were placed in the humid room and in the laboratory to determine weight loss as a function of time.

CHAPTER 3

MATERIAL DESCRIPTIONS AND SPECIAL TESTS

3.1 TUNNEL U12e-12 TUFF

The tuff material from Tunnel U12e-12 arrived in two separate shipments as previously noted. The cores in the first batch were covered by a blue dye, used during field coring operation to determine drill-water penetration. Penetration into the core by the dye was minimal (<25 mils) except in the broken pieces, which may have been fractured during coring. The blue dye was not present on those specimens received in the second shipment.

Table 3.1 lists all the U12e-12 specimens and shows the boring number and location of each core as recorded from the shipping tag. The core came from the left rib of Tunnel U12e-12 at the following distances from the HUDSON MOON working point: DB7A, 1,306 feet; DB7B, 1,300 feet; and Site B, 1,301-1,307 feet. Also given in Table 3.1 is a physical description of each core, the as-received water contents and wet unit weights, the exposed water contents and wet unit weights, and the dry unit weights, γ_d . Dry unit weight is the ratio of dry specimen weight to intact specimen volume and can be calculated from:

$$\gamma_d = \frac{Y}{1 + w} \quad (3.1)$$

The U12e-12 specimens could be classified in two groupings based on physical appearance and cementation. Three of the specimens, E12.7B.8.0, E12.7B.8.6, and E12.7B.10.2, were white in color and contained white nodules with black and brown specks. The specimens were not friable. The average as-received water content for those specimens was 25.3 percent, and the average wet unit weight was 1.87 g/cm^3 . The rest of the specimens from Tunnel U12e-12, Boring DB7A, and Site B, were, in general, dirty cream or yellowish in color with white nodules and black and brown specks. The specimens were very friable. The as-received water contents ranged from 25 to 29 percent and the wet unit weights ranged from

1.85 to 1.89 g/cm³. However, groups of specimens from Tunnel U12e-12 were white in color when dry.

3.2. TUNNEL U12n-06 TUFF

Five U12n-06 tuff specimens were received by WES in the second shipment. Table 3.2 lists those specimens by boring and location. In addition, Table 3.2 lists the specimen descriptions, as-received water contents and wet unit weights, the exposed water contents and wet unit weights, and the dry unit weights. In Tunnel U12n-06, Boring DB2 came from the right rib at a distance of 786 feet from the DIANA MIST working point.

The U12n-06 specimens could be divided into two groups based on color. None of the specimens were friable. Specimens N06.2.26.0, N06.2.26.7, and N06.2.27.0 were red in color with white nodules and some black and brown specks. The average as-received water content and wet unit weight were 22.0 percent and 1.91 g/cm³, respectively. The specimens dried to a light pink color. Specimens N06.2.31.0 and N06.2.31.5 were fine grained, gray in color with some yellow-colored, coarse-grained zones. Black and brown specks were more prevalent in the yellow-colored zones. Specimen N06.2.31.0 was loaded to failure in a shear test and the failure zone appeared to concentrate in the yellow-colored portion of that specimen. Thus, this color may be a significant index property. Both specimens dried to an off-white color. The zone that was originally yellow dried to a slightly different shade of off white than did the gray material. The as-received water content and wet unit weight of Specimen N06.2.31.0 were 18.6 percent and 1.95 g/cm³, while those for Specimen N06.2.31.5 were 16.2 percent and 2.00 g/cm³, respectively. It appeared that the presence of gray material correlates with the lower water contents and higher densities.

3.3 SPECIAL TESTS ON U12e-12 TUFF

Several of the fractured yellowish-colored specimens were used to study the effect of handling on water content. Each core was removed from its wrappings and weighed. Some core pieces were placed in the

humid room. At various intervals of time, they were quickly removed, weighed, and placed back in the humid room. Figure 3.1 shows a plot of specimen weight versus time for Specimen E12.SB.15.0. It indicates that the tuff will lose water even under 95 to 100 percent relative humidity conditions. The average relative humidity was approximately 97 percent over the duration of the test. Specimen pieces from Core E12.SB.17.4 were allowed to remain exposed in the laboratory at an average relative humidity of 72 percent. A plot of that specimen's weight versus time is also shown in Figure 3.1. The results indicate a continued loss of water of the tuff when exposed and probably explain the slight loss in specimen weight observed after triaxial testing.

A piece from Specimen E12.SB.10.7 was placed in a drying oven at approximately 110 C. The results were plotted as specimen weight versus time as shown in Figure 3.1. This plot indicates that the tuff lost most of its free water during the first two hours in an oven, but required a much longer period to drive out the remaining trapped free water.

3.4 SPECIAL TESTS ON U12n-06 TUFF

A study of the effect of handling on water content was also conducted on specimen pieces from Specimen N06.2.26.0. The study was similar to that conducted on the U12e-12 tuff. The specimen pieces were placed in the humid room and in the laboratory. The data for the two conditions plotted as specimen weight versus time are shown in Figure 3.1. The results indicate the same trend that was observed for the U12e-12 tuff. The U12n-06 tuff lost water in a nearly 100 percent humidity environment. The tuff continued to lose water when exposed in the laboratory.

3.5 COMPARISON BETWEEN U12e-12 AND U12n-06 TUFF

In addition to variations in physical appearance, other differences between the U12e-12 and U12n-06 tuffs were noted. Figure 3.2 is a plot of dry unit weight versus as-received water content for both tuffs. As can be seen, the U12n-06 tuff had higher dry unit weights and lower

water contents than the U12e-12 tuff. The U12n-06 tuff also appeared to be less friable than the U12e-12 tuff.

Four Brazilian tensile tests³ were conducted and the results are shown in bar-graph form, Figure 3.3. The U12n-06 tuff specimen had the greatest tensile strength, -270 psi. Core pieces from Specimen E12.SB.15.0 had an average tensile strength of -160 psi. The higher tensile strength of the tuff from Tunnel U12n-06 correlates with its less friable nature. One test was also conducted on Specimen E12.SB.9.6, which had previously been tested to failure in the triaxial shear test. Its peak tensile strength was -60 psi, indicating a marked loss in tensile strength, when compared with a similar tuff, E12.SB.15.0, that had not been subjected to triaxial loading.

³ U. S. Army Engineer Waterways Experiment Station, CE; "Handbook for Concrete and Cement"; Test Standard CRD 77-70; August 1949 (with quarterly supplements); Vicksburg, Mississippi.

TABLE 3.1 COMPOSITION PROPERTIES OF TUNNEL U12e-12 TUFF

Specimens from Borings DB7B and DB7A received 5/27/71; Site B received 7/9/71.

Boring	Location (Distance Drilled into Tun- nel Wall)	WEC Specimen Number	Material Description	As Received		Exposed		Dry Unit Weight γ_d	Remarks ^a
				Water Content w	Wet Unit Weight γ	Water Content w	Wet Unit Weight γ		
	feet			percent	g/cm ³	percent	g/cm ³	g/cm ³	
DB7B	8.0-8.5	E12.7B.8.0	White with brown and black specks	24.6	1.88	24.4	1.88	1.51	H _D and S _D
DB7B	8.6-9.1	E12.7B.8.6	White with brown and black specks	25.4	1.86	25.3	1.86	1.48	H _S and S _S
DB7B	10.2-10.7	E12.7B.10.2	White with brown and black specks	25.9	1.87	25.8	1.86	1.49	H _D and S _D
DB7A	7.0-7.5	E12.7A.7.0	Yellowish or dirty cream with brown and black specks; red color at bottom, friable	25.8	--	--	--	--	Broken
				28.3	--	--	--	--	--
DB7A	7.5-8.0	E12.7A.7.5	Yellowish with brown and black specks, friable	29.4	--	28.1	1.85 ^b	1.44	Broken
				29.1	--	--	--	--	--
Site B 2+96.07	9.1	E12.SB.9.1	Yellowish with brown and black specks, friable	24.9	1.88	24.3	1.87	1.51	H _D
Site B	9.6	E12.SB.9.6	Yellowish with white nodules, brown and black specks, friable	--	1.89	22.8	1.88 ^b	1.53	H _S and S _S horizontal break
Site B 2+96.07	10.7	E12.SB.10.7	Yellowish with white nodules, brown and black specks, friable	27.2	1.86 ^b	--	--	1.46	Broken
Site B 2+94.07	15.0	E12.SB.15.0	Yellowish with white nodules, brown and black specks, friable	--	--	26.0 24.5 (Longer exposure)	--	--	Broken
Site B 2+96.07	16.3	E12.SB.16.5	Yellowish with white nodules, brown and black specks, friable	24.3	1.88	23.8	1.87	1.51	H _D and S _D
Site B 2+99.07	17.4	E12.SB.17.4	Yellowish with white nodules, brown and black specks, friable	28.2	--	--	--	--	Broken
				26.0	--	--	--	--	--
Site B	18.0	E12.SB.18.0	Yellowish with white nodules, brown and black specks, friable	28.3	1.85 ^b	--	--	1.44	Broken

^a Definition of terms: H_S = static hydrostatic test; H_D = dynamic hydrostatic test; S_S = static shear test; S_D = dynamic shear test.^b Density determined by mercury-displacement method.

TABLE 3.2 COMPOSITION PROPERTIES OF TUNNEL UL2h-06 TUFF

Specimens received 7/9/71.

Boring	Location (Distance Drilled into Tun- nel Wall)	WES Specimen Number	Material Description	As Received		Exposed		Dry		Remarks ^a
				Water Content w	Wet Unit Weight γ	Water Content w	Wet Unit Weight γ	Unit Weight γ_d	Unit Weight γ	
	feet			percent	g/cm^3	percent	g/cm^3	g/cm^3	g/cm^3	
DB2 10+10.04	26.0	NO6.2.26.0	Red with white nodules, black and brown specks	--	1.93 ^b	20.2	--	--	--	Broken
DB2 10+10.04	26.7	NO6.2.26.7	Red with white nodules, black and brown specks	--	1.91	--	--	--	--	H _s and S _s
DB2 10+10.04	27.0	NO6.2.27.0	Red with white nodules, black and brown specks	22.0	1.90	21.6	1.90	1.56	1.56	H _D and S _D
DB2	31.0	NO6.2.31.0	Gray material, some yellow with brown and black specks	18.6	1.95	--	--	1.64	1.64	H _D and S _D
DB2 10+10.04	31.5	NO6.2.31.5	Gray material, some yellow with brown and black specks	16.2	2.00	16.0	2.00	1.72	1.72	H _D

^a Definition of terms: H_s = static hydrostatic test; H_D = dynamic hydrostatic test; S_s = static shear test; S_D = dynamic shear test.

^b Density determined by mercury-displacement method.

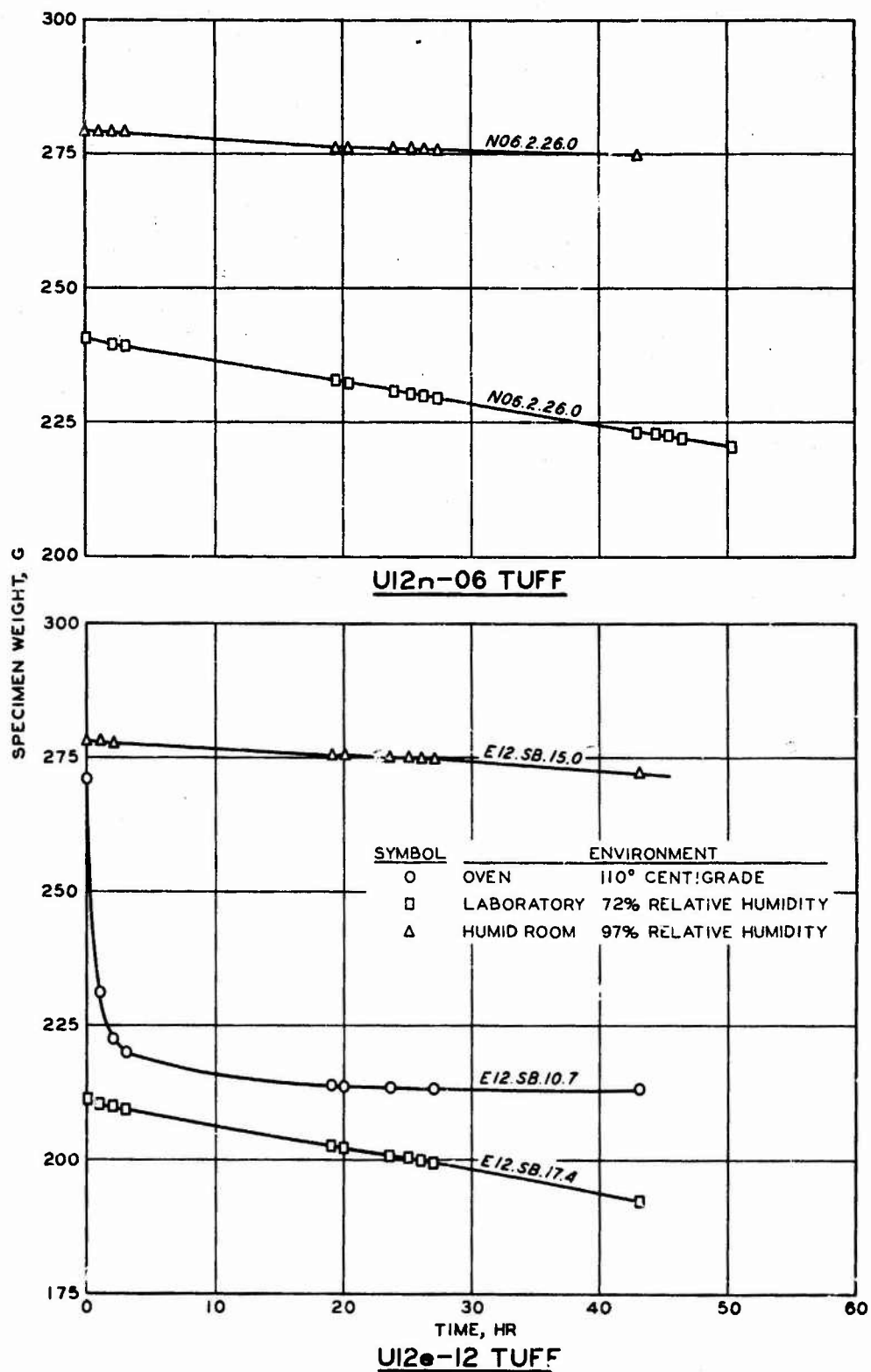


Figure 3.1 Specimen weight versus time for five pieces of tuff placed in three different environments.

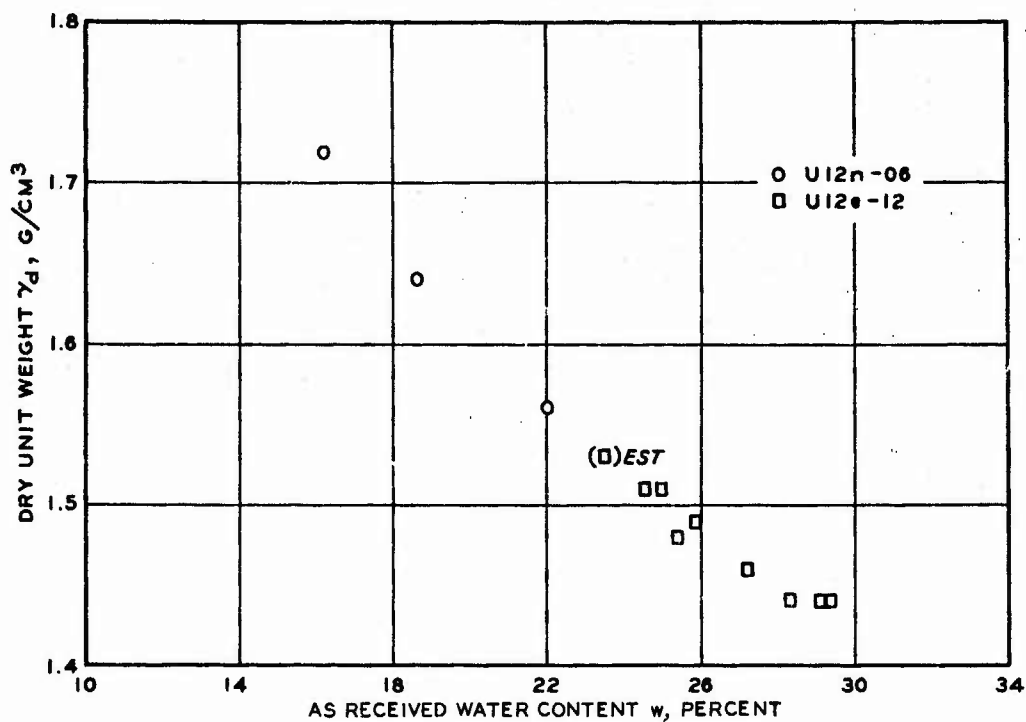


Figure 3.2 Dry unit weight versus water content for tuft from Tunnels U12e-12 and U12n-06.

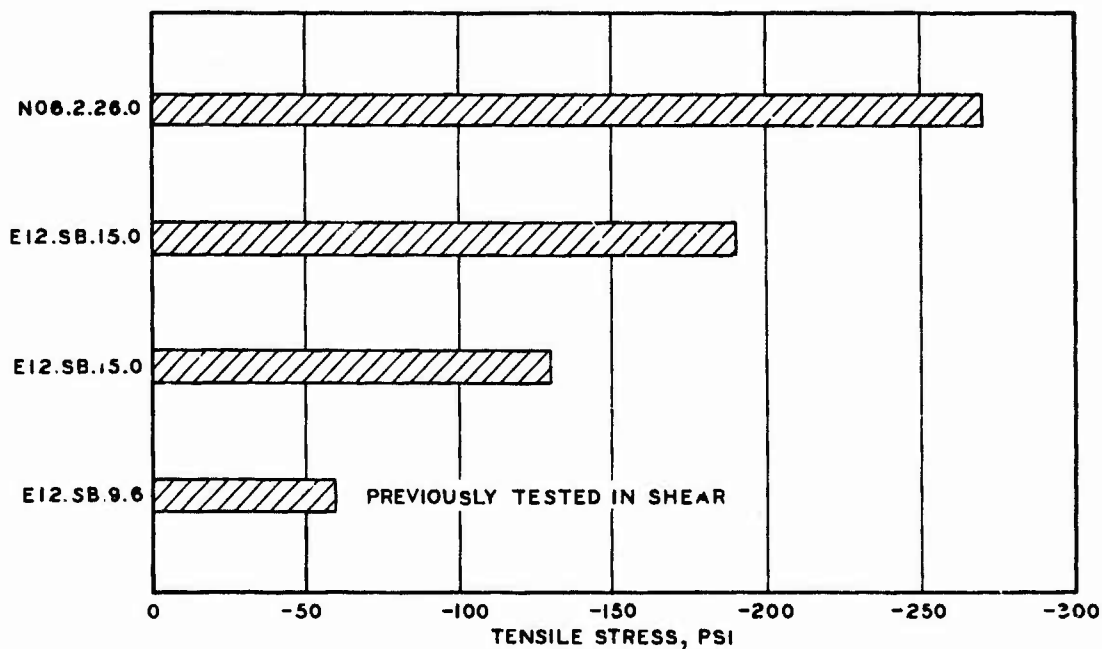


Figure 3.3 Brazilian tensile tests.

CHAPTER 4

CONSTITUTIVE PROPERTY TESTS ON TUNNEL U12e-12 TUFF

Only five of the twelve specimens received by WES were intact and unfractured and were, therefore, suitable for testing. One of the broken specimens, E12.SB.9.6, was tested, however, because it had a clean horizontal break through the center of the specimen and could be pieced back together. The data from this specimen could be suspect. Another specimen, E12.SB.9.1, contained a small crack near the core end, but remained intact. Specimens E12.7B.8.6 and E12.SB.9.6 were loaded statically for both hydrostatic and shear tests. Specimens E12.7B.8.0, E12.7B.10.2, and E12.SB.16.5 were loaded dynamically for both hydrostatic and shear tests; Specimen E12.SB.9.1 was loaded and unloaded in dynamic hydrostatic compression. As previously observed, the specimen from Boring DB7B was different in appearance from the specimens from Borings DB7A and Site B.

4.1 HYDROSTATIC TESTS

The results of the hydrostatic tests are presented in Figures 4.1 and 4.2 as plots of mean normal stress p versus the axial strain ϵ_a and radial strain ϵ_r . The test results of the white-colored specimens from Boring DB7B are shown in Figure 4.1. It should be noted that the internal axial deformation measurement unit was not working properly during test on Specimen E12.7B.10.2. Therefore, only the radial strain could be determined in that test. The results of the three tests were consistent. The data indicate a nearly isotropic behavior of the material since there were only slight differences between the radial and axial strain increments above 1,000 psi. At low stress levels (<500 psi) the axial strain of Specimen E12.7B.8.6 may be in error due to top-cap seating, which would result in larger strain. Also, since the cores were removed at some depth in the field, small microfractures could have opened within the rock due to removal of the overburden pressure. The laboratory tests were begun under atmospheric pressure; some additional pressure (equivalent to the overburden stress) might have been required

to close those fractures. The reapplication of pressure equivalent to the in situ overburden stress may have resulted in some initial straining. However, the individual effects could not be assessed with the available data; therefore, the test data reported herein have not been rezeroed, unless so indicated.

The results from the tests conducted on the yellowish-colored material, the Site B tuff, are shown in Figure 4.2. The data show approximately the same axial strain increment versus pressure increment relation at higher stress as was noted for the Boring DB7B tuff. The relatively large amounts of initial axial strain at low pressures (<1,000 psi) of Specimen E12.SB.9.1 and especially E12.SB.9.6 were probably caused by the closure of a horizontal crack and break in the respective specimens. Note that the axial strain of Specimen E12.SB.9.6 has been shifted by 0.3 percent to fit on the plot in Figure 4.2. The radial strain responses of the three specimens from Site B were very different from those of the Boring DB7B tuff. The radial strain increment for an increment of p is much greater than the axial strain increment, indicating a marked anisotropic behavior of that material. Since the cores were taken along a horizontal plane in the tunnel, the radial direction of the specimens corresponds to the vertical direction in the field.

The results of all the hydrostatic tests on specimens from both Boring DB7B and the Site B material are shown in Figure 4.3 as a plot of mean normal stress versus volumetric strain. The slope of the curves is the bulk modulus K . The average tangent K above 1,000-psi pressure of the Boring DB7B material is approximately 1.2×10^6 psi. The Site B material appears to have an average K of 390×10^3 psi over the same pressure range. The Boring DB7B material does not appear to be sensitive to loading rate during hydrostatic loading. The results of the three tests conducted on the Site B material indicate more experimental scatter; in fact, the two dynamic loadings may have a lower K than the static test. From the available data, the effect of loading rate on bulk modulus can only be estimated, but these data do suggest that stress rate effects on the bulk modulus are small.

4.2 SHEAR TESTS

The results of each shear test conducted on the tuff are presented in Figures 4.4 through 4.8 as plots of principal stress difference versus axial and radial strain. In three of the tests, shown in Figures 4.4, 4.5, and 4.6, the axial strain during the initial loading portion was rezeroed, but the actual data are still shown as a dashed line in each figure. The data, in general, showed little hysteretic behavior of the material during loading prior to failure. The unloading-reloading slopes of the principal stress difference axial strain and radial strain curves appeared equal to the initial loading slopes. The average axial strain at peak stress for all the tests was approximately 1.25 percent. The radial strain at failure varied more than the axial strain and indicated some loading-rate effect. The radial strain at failure for the dynamic tests was less than that for the static tests. The material continued to strain both axially and radially after peak stress, with a slight decrease in principal stress difference.

Figure 4.9 is a plot of principal stress difference $\sigma_a - \sigma_r$ versus principal strain difference $\epsilon_a - \epsilon_r$ showing the results of all the shear tests. The slope of these curves is $2G$ (G is the shear modulus). Although apparent experimental scatter existed, the trend indicates a loading-rate effect on shear modulus. Dynamic tests on Specimens E12.7B.8.0 and E12.SB.16.5, with 2- and 3-msec loading times to peak stress, respectively, indicate an average initial shear modulus G of 1.2×10^6 psi. The high value of G does not appear to be consistent with the average values of bulk modulus K of 1.2×10^6 psi. According to elastic theory, when $G = K$, Poisson's ratio becomes 0.125. It should be noted, however, the values of initial radial strain measured in the triaxial shear test tend to give low or even negative values of Poisson's ratio. The slower dynamic test on Specimen E12.7B.10.2, with 32 msec to peak, and the static test on Specimen E12.7B.8.6, with 60 seconds to peak, indicate an average initial shear modulus of 490×10^3 psi. The value of $G = 490 \times 10^3$ psi is more consistent with the average value of K and would give a Poisson's ratio of 0.32, which

appears reasonable. The specimen with the horizontal break had the lowest shear modulus, i.e. 220×10^3 psi. It is not known if the horizontal break caused the low value or if the value is more representative of the Site B material. Since the average bulk modulus for the Site B material was 390×10^3 psi, a small value of G , such as 220×10^3 psi, would yield a more reasonable value of Poisson's ratio. Other factors, such as the effect of mean normal pressure on shear modulus, were not evaluated; therefore, the results should be used only in a qualitative manner.

The peak principal stress difference from each of the five shear tests is plotted versus mean normal stress in Figure 4.10. The loading path of each test is shown in the figure as a dashed line. All the tests were conducted with a constant confining pressure except the test on Specimen E12.7B.10.2, which was conducted with a constant stress ratio, σ_r/σ_a of 0.11. The data appear to indicate experimental scatter; however, the dynamic tests have a somewhat higher principal stress difference at failure than do the static tests. If the Boring DB7B material has a different strength or yield envelope than the Site B material, then the data may be considered separately. The ratio of peak dynamic strength to static strength could be as great as 1.3 for the DB7B material based on a comparison of the results of the two tests with 2 msec and 60 seconds times to peak. The strength ratio for the Site B material could be as great as 1.28 based on the comparison of the results of the two tests with loading times of 3 msec and 66 seconds.

It should be noted that the symbols shown at various increments on each of the hydrostatic and shear test plots are not actual data points, but are for identification purposes only.

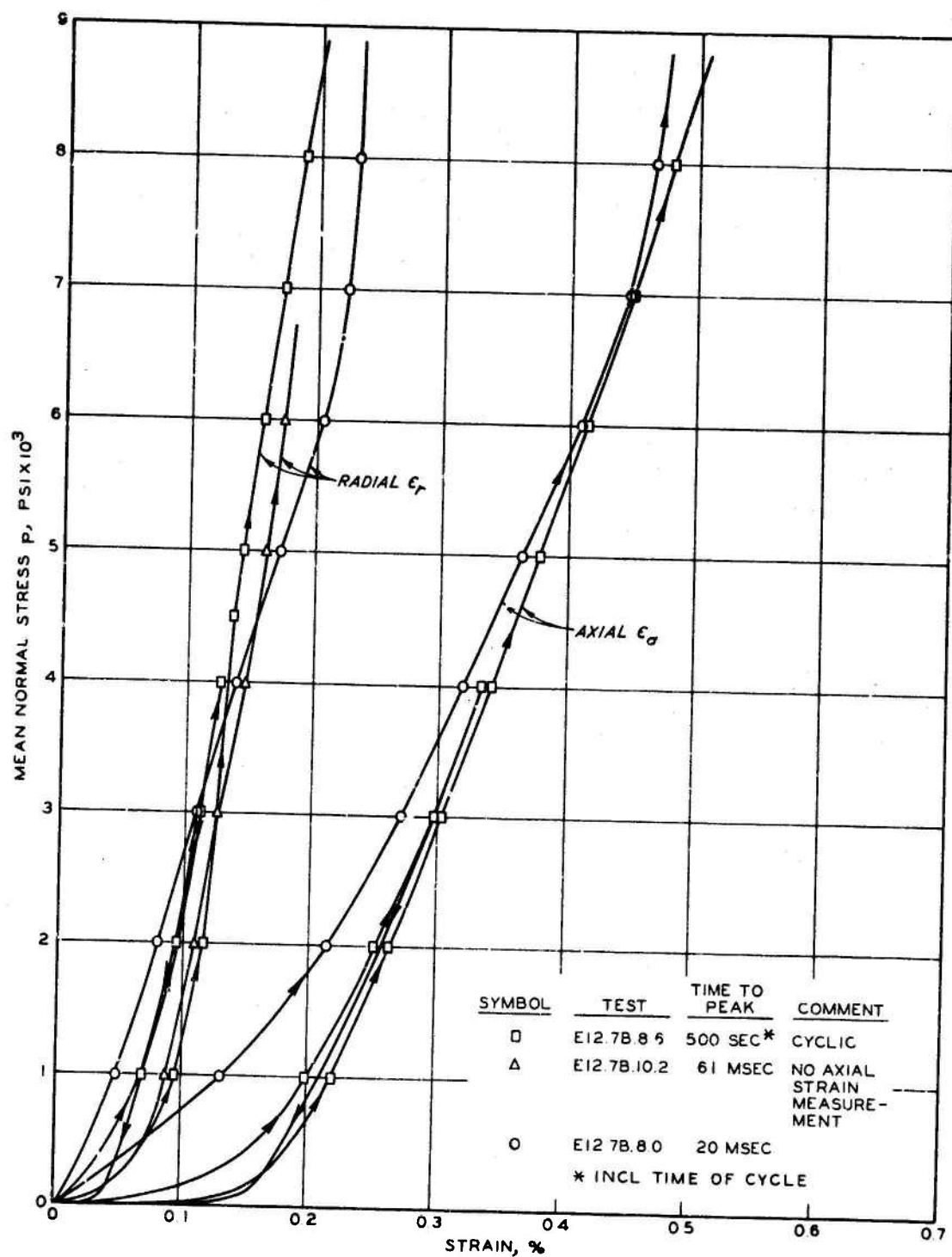


Figure 4.1 Stress-strain data from hydrostatic tests conducted on tuff from Tunnel U12e-12, Boring 7B.

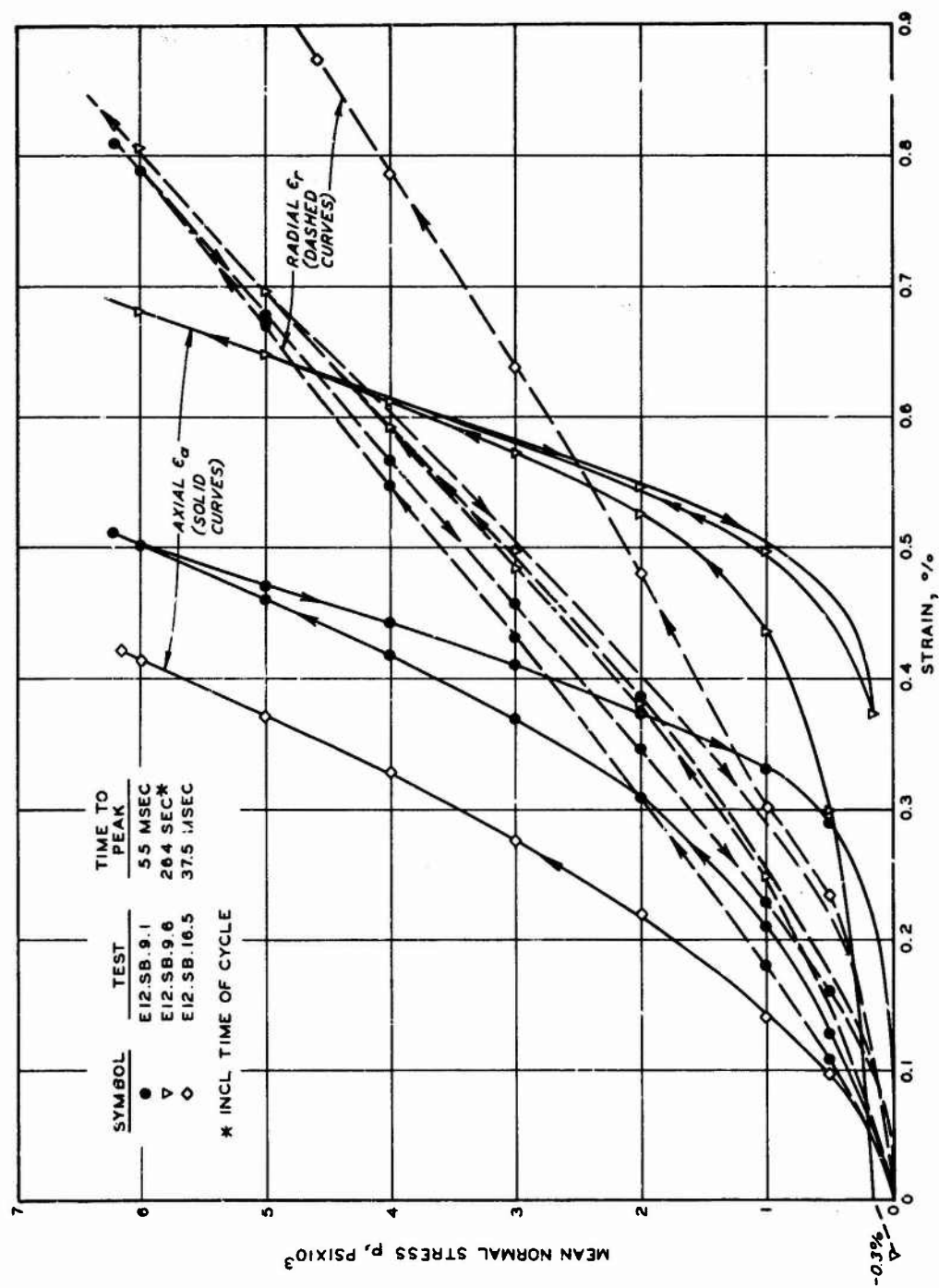


Figure 4.2 Stress-strain data from hydrostatic tests conducted on tuff from Tunnel U12e-12, Site B.

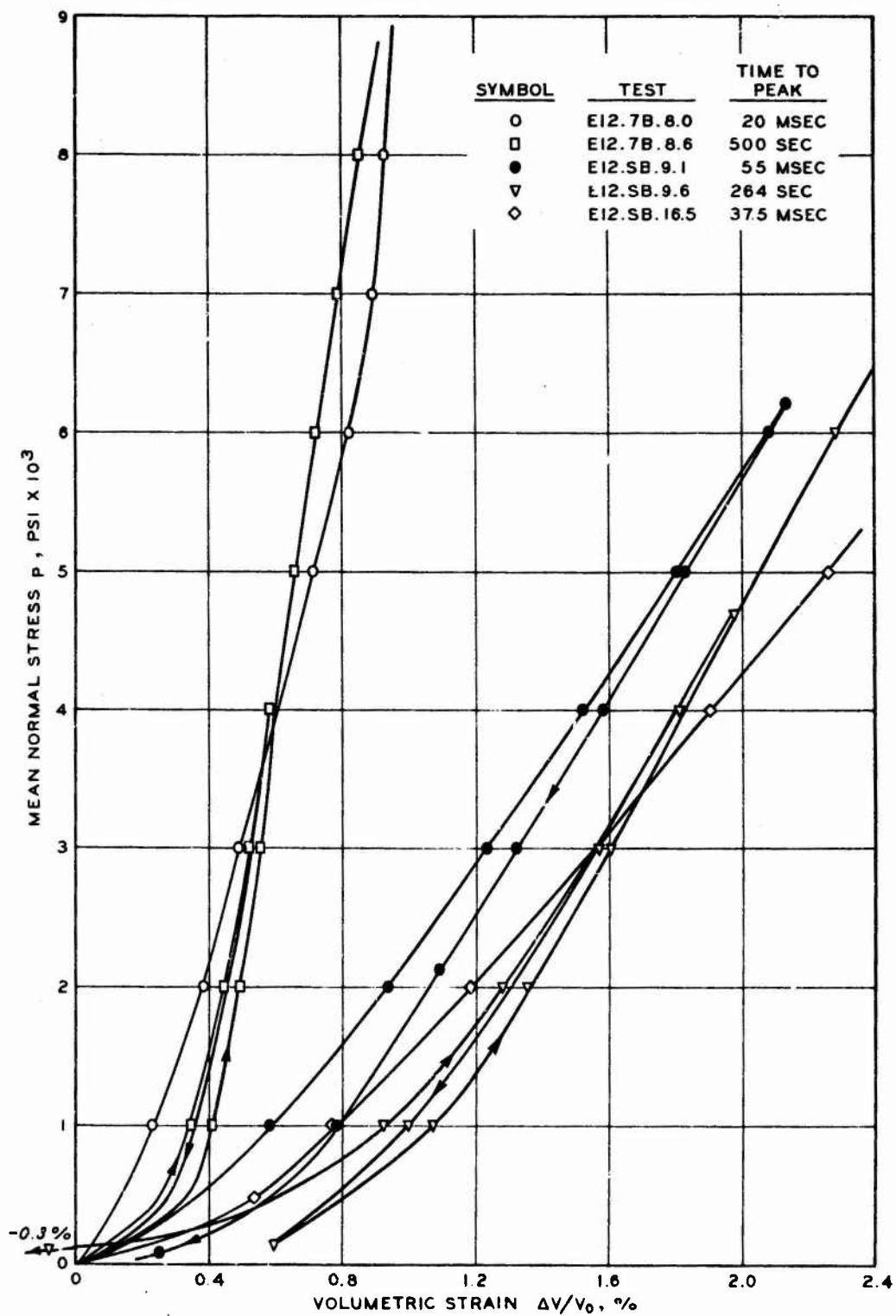


Figure 4.3 Stress versus volumetric strain showing the hydrostatic response of tuff from Tunnel U12e-12.

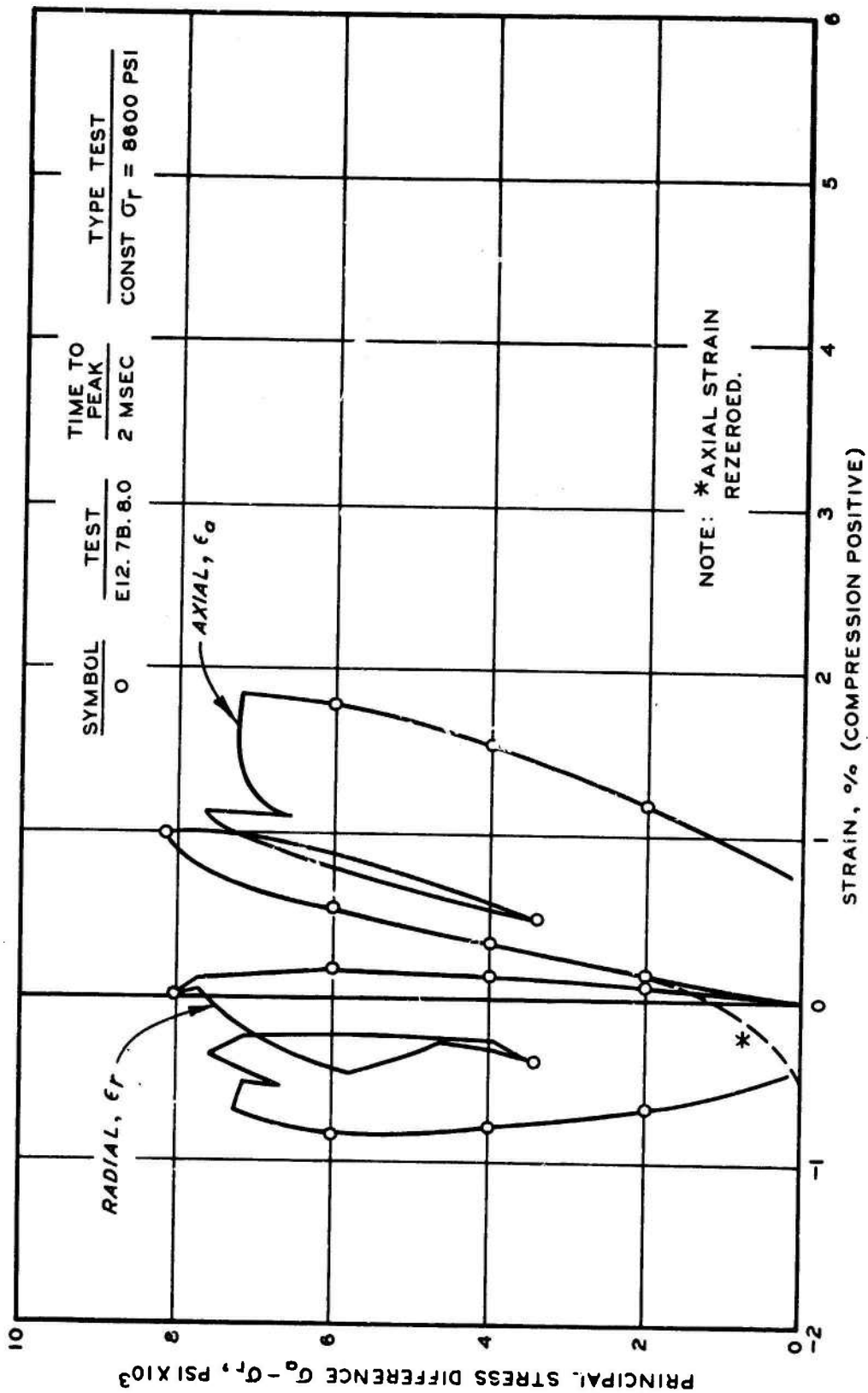


Figure 4.4 Shear test results from Test E12.7B.8.0 showing axial and radial strain response.

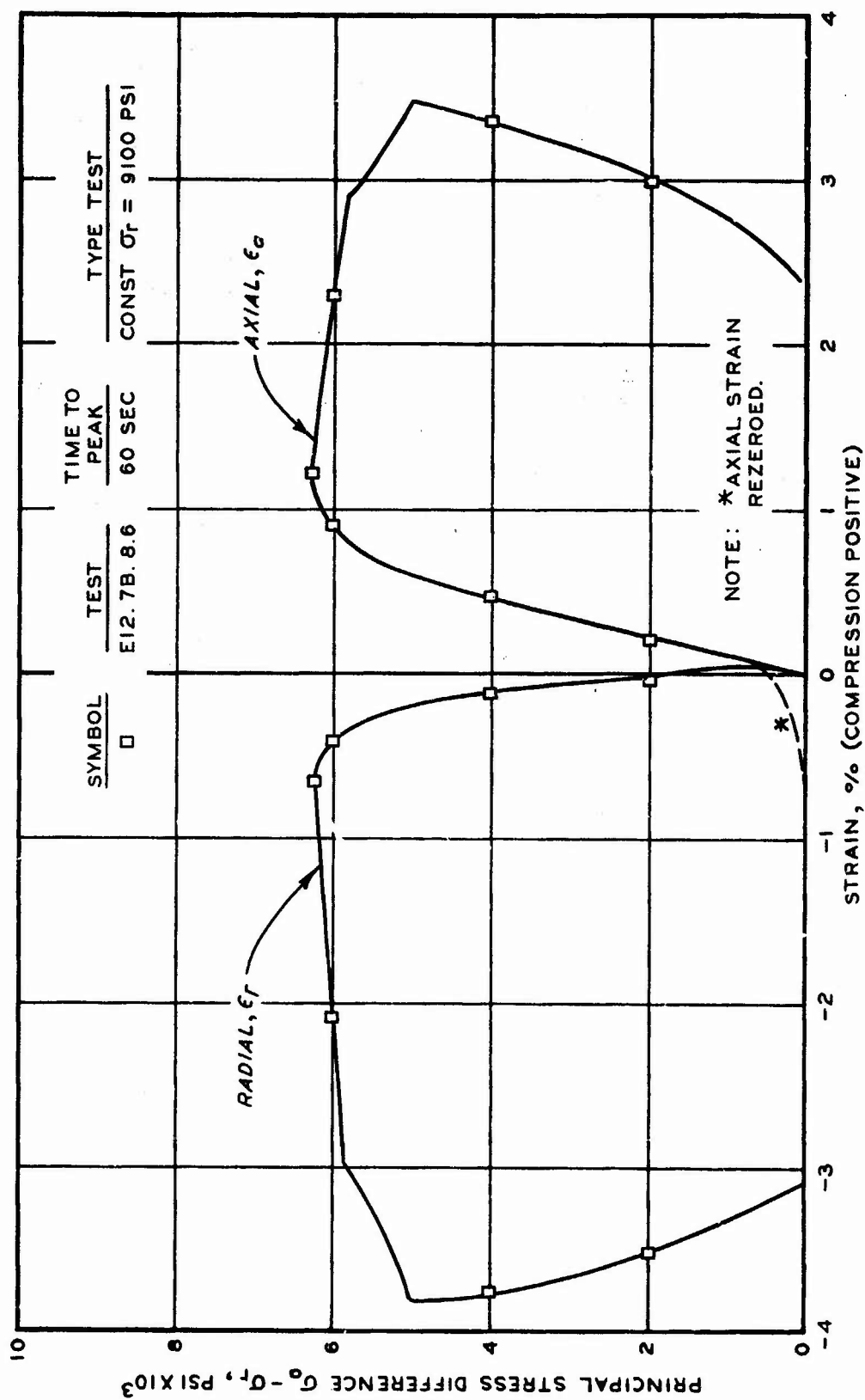


Figure 4.5 Shear test results from Test E12.7B.8.6 showing axial and radial strain response.

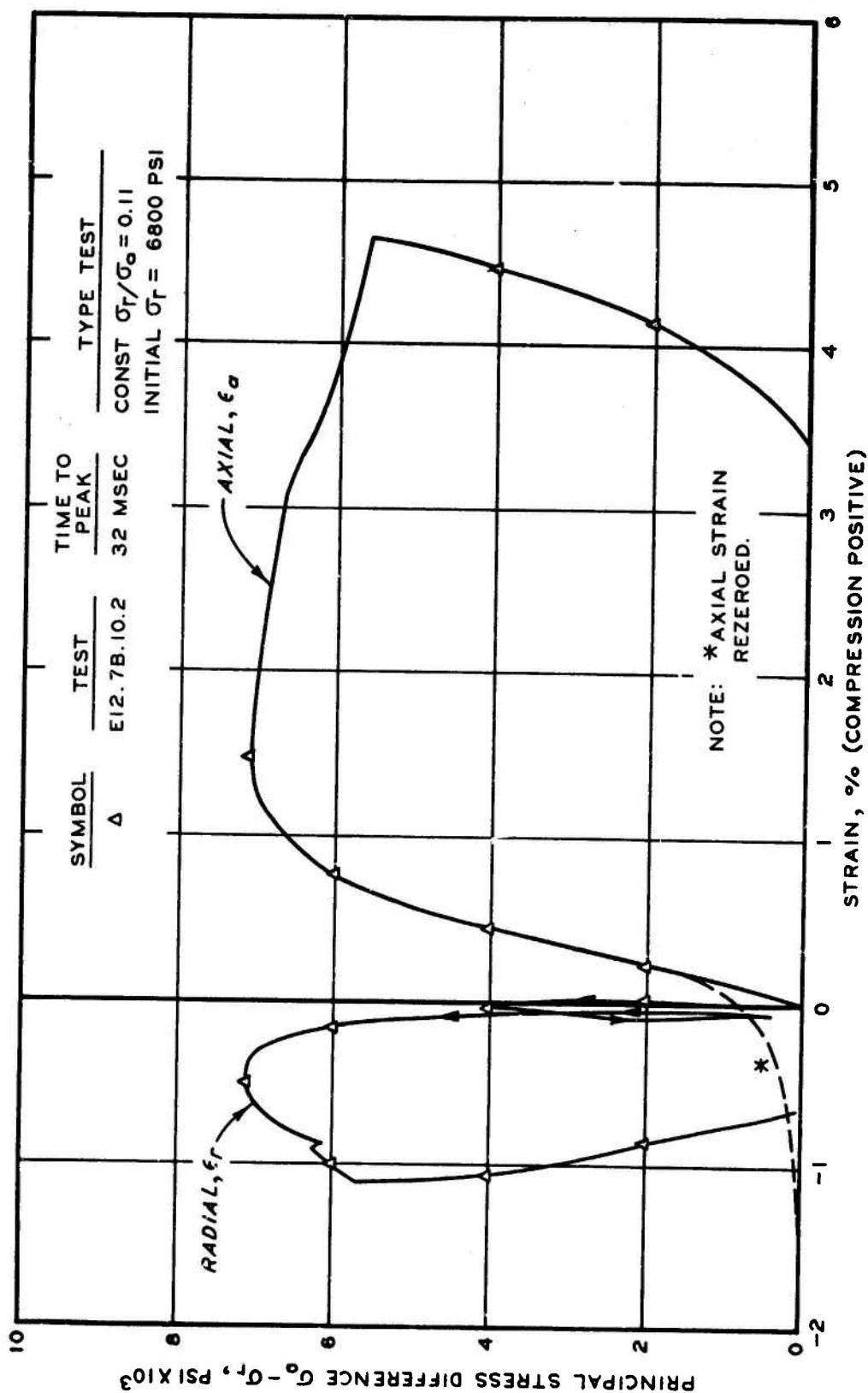


Figure 4.6 Shear test results from Test E12.7B.10.2 showing axial and radial strain response.

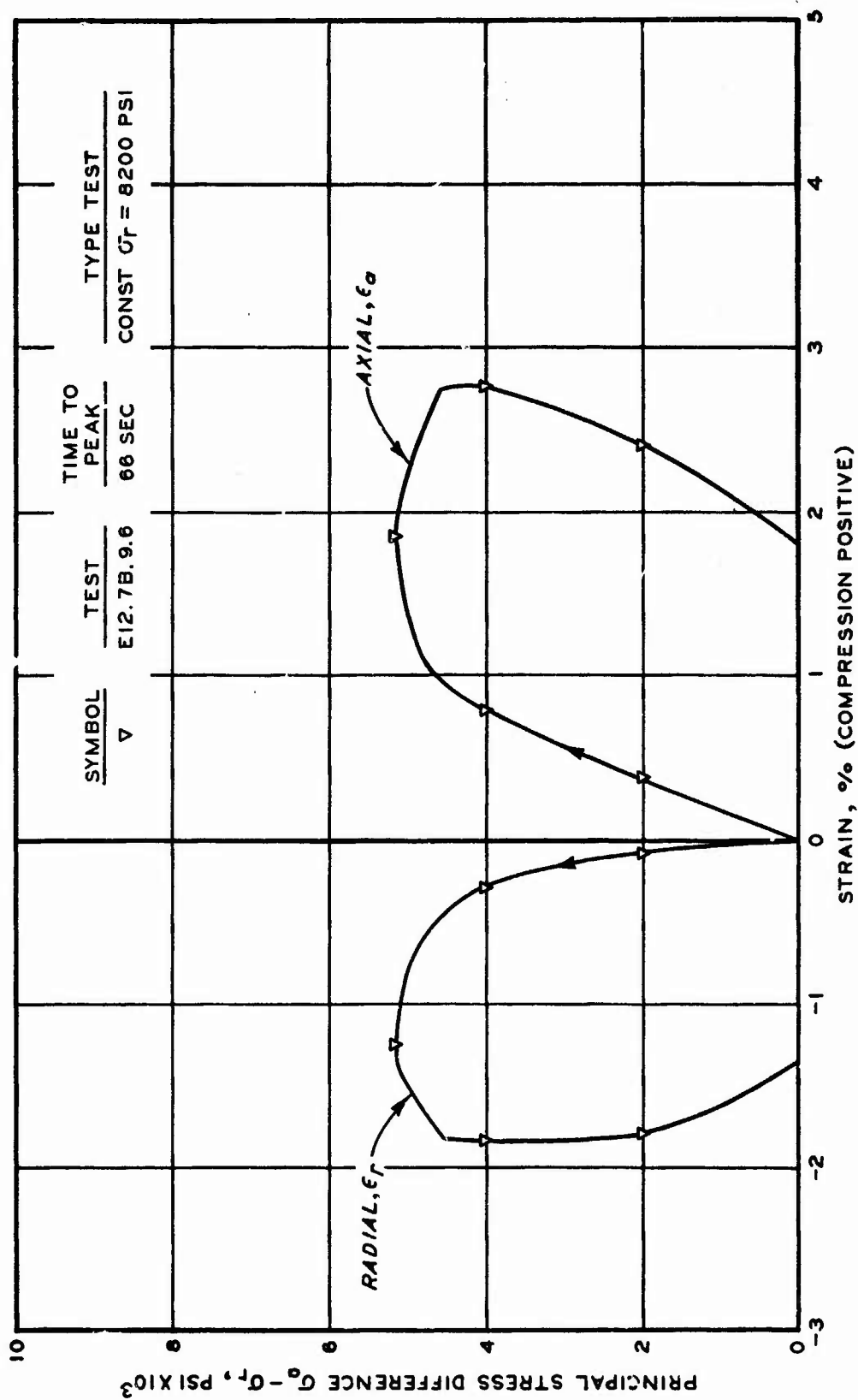


Figure 4.7 Shear test results from Test E12.SB.9.6 showing axial and radial strain response.

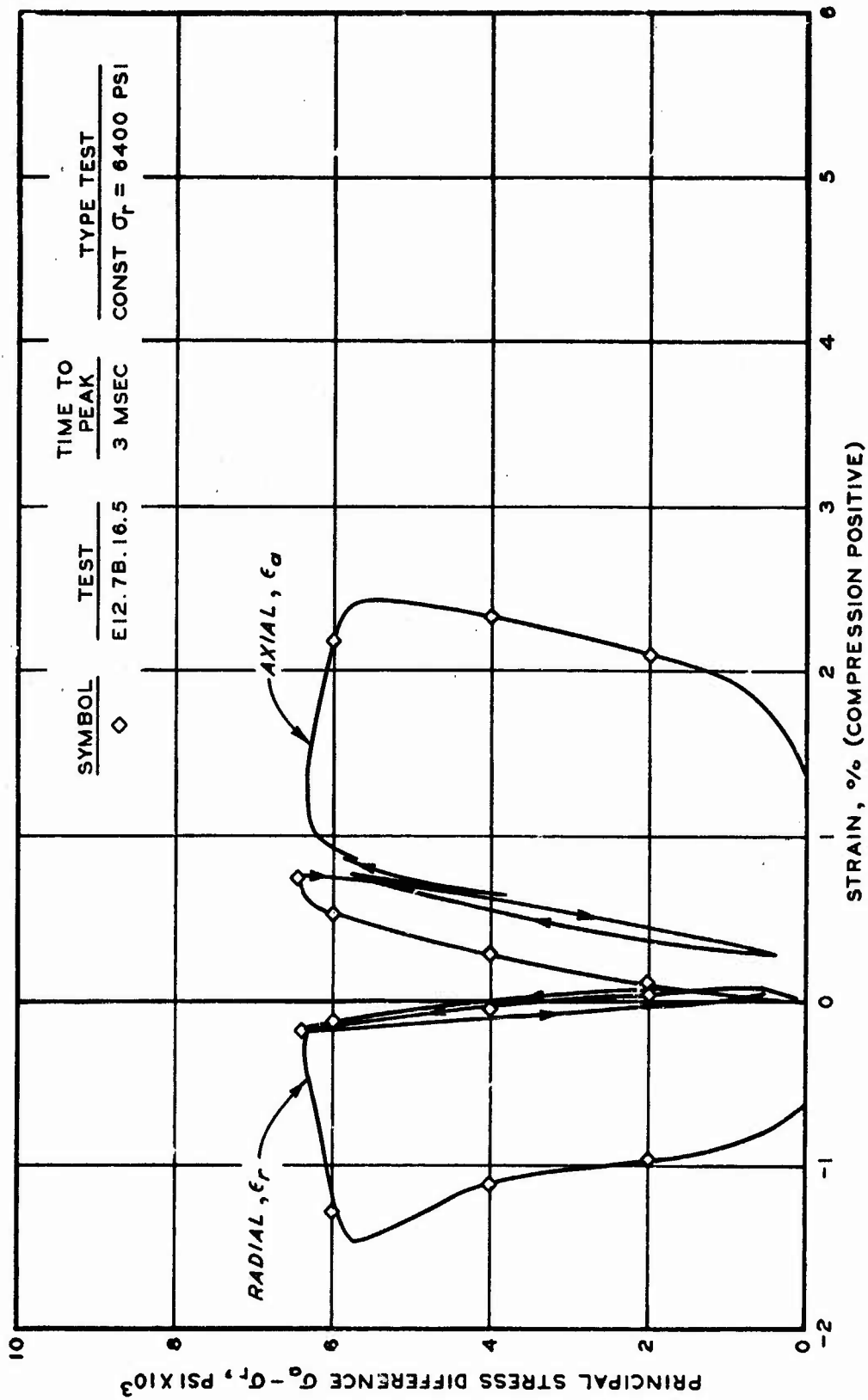


Figure 4.8 Shear test results from Test E12.SB.16.5 showing axial and radial strain response.

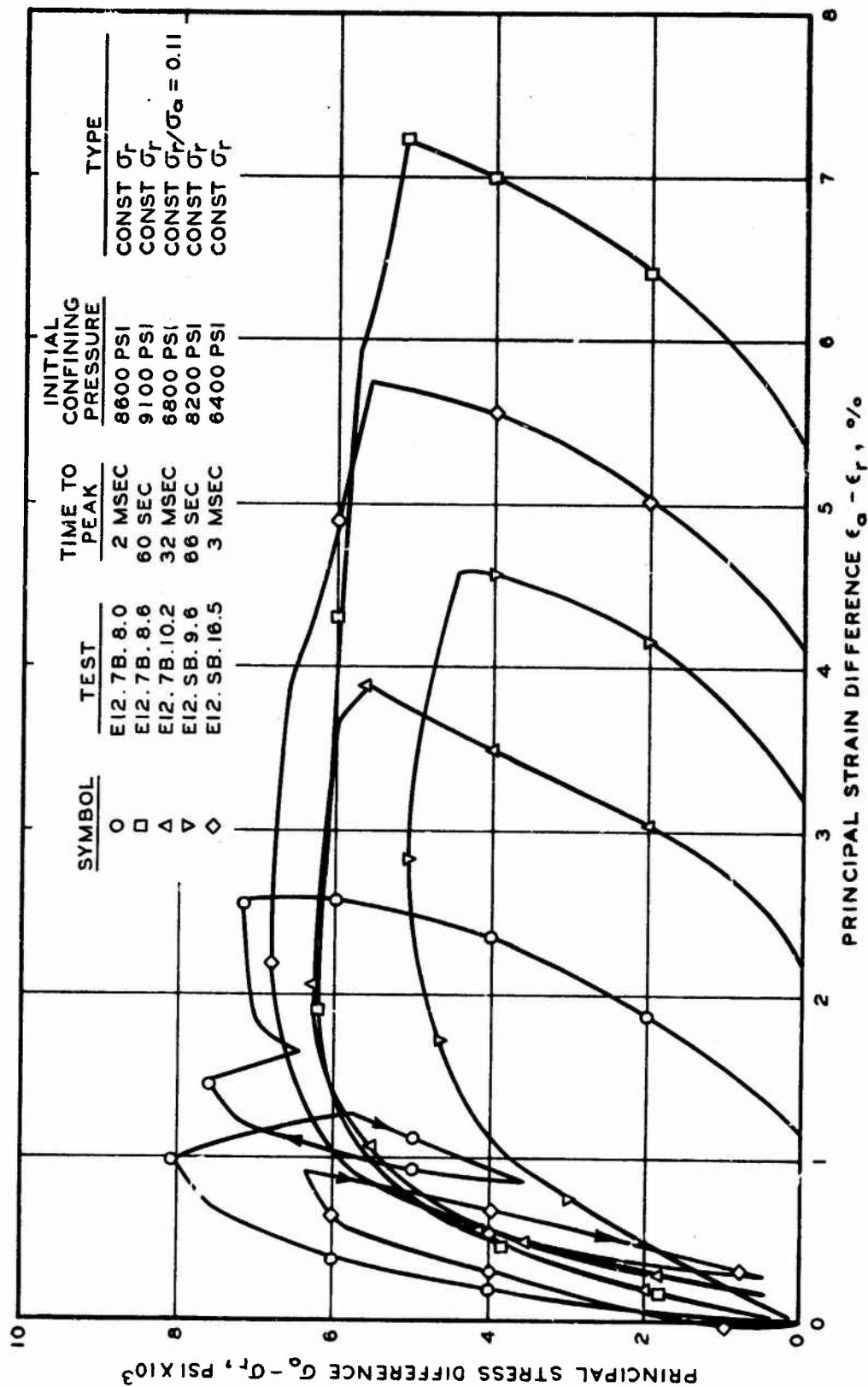


Figure 4.9 Principal stress difference versus principal strain difference showing results from shear tests conducted on tuff from Tunnel U12e-12.

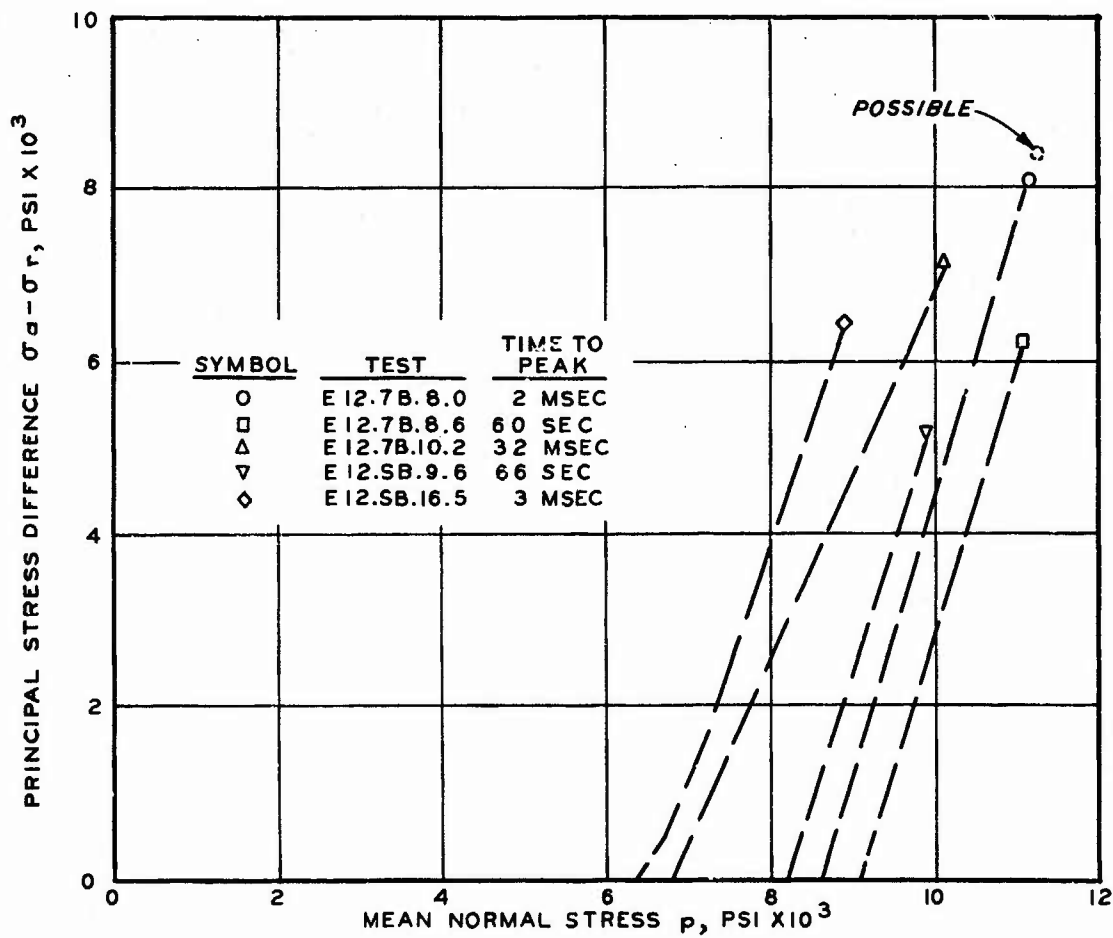


Figure 4.10 Principal stress difference versus mean normal stress showing peak stresses from five shear tests on tuff from Tunnel U12e-12.

CHAPTER 5

CONSTITUTIVE PROPERTY TESTS ON U12n-06 TUFF

Four of the five U12n-06 tuff specimens received by WES were tested in the DHT. Specimen N06.2.26.0 arrived at WES in a broken condition and could not be tested. Of the four remaining specimens, Specimen N06.2.26.7 was loaded statically, both hydrostatically and in shear. Specimens N06.2.27.0, N06.2.31.0, and N06.2.31.5 were loaded dynamically in hydrostatic compression. Specimens N06.2.27.0 and N06.2.31.0 were also loaded dynamically in shear following hydrostatic loading. As described in Section 3.2, Specimens N06.2.26.0, N06.2.26.7, and N06.2.27.0 were red in color, and Specimens N06.2.31.0 and N06.2.31.5 were gray and yellow.

5.1 HYDROSTATIC TESTS

The results of all the hydrostatic tests are shown in Figure 5.1 as a plot of mean normal stress p versus axial and radial strains. Except for Specimen N06.2.31.5, there is little variation in the data. Specimen N06.2.31.5 was tested twice; only the data from the second loading are shown in Figure 5.1. The data in the first loading were lost due to an electrical short in the measurement system. The difference between the data for this specimen and those for the others may be related to the reloading response characteristics of the tuff or to the fact that Specimen N06.2.31.5 may have been taken from a different material. As previously noted, Specimen N06.2.31.5 was gray in color and had a high unit weight and low water content. However, the test results on Specimen N06.2.31.0, which also contained some gray zones and had a high unit weight, agreed with the results from other tests. The results of the test in which the pressure was cycled, Test N06.2.26.7, indicate that there is little hysteretic response in the tuff. In the test on Specimen N06.2.27.0, there is a decrease in slope at a pressure level of 5,000 to 5,500 psi. It is not known if this was caused by a structural collapse or by void closure within the specimen.

A large amount of axial strain was measured during application of

the first 500 psi in all the tests. A portion of that strain could have been caused by top-cap seating error and/or by an effect due to reapplication of pressure equal to the natural overburden stress, as previously mentioned in Chapter 4.

The results of the hydrostatic tests were replotted as mean normal stress p versus volumetric strain $\Delta V/V_0$, and these plots are shown in Figure 5.2. Except for the first 500 psi, the slopes of the $\Delta V/V_0$ curves, which represent the bulk moduli K , compare favorably, and the average tangent value of K above 1,000 psi is 1.2×10^6 psi. Specimen N06.2.31.5, which had a different axial-radial strain response from all the other specimens, appears to have about the same bulk modulus as the others except for the amount of initial strain. Very little difference was noted between the unloading-reloading response and the initial loading. It also may be noted that the one static test on Specimen N06.2.26.7 does not appear to differ from the three dynamic tests. Based on these limited results, the tuff from Tunnel U12n-06 does not appear to have significant loading-rate effects under hydrostatic loading.

5.2 SHEAR TESTS

The results of the three triaxial shear tests are shown in Figure 5.3 through 5.5 as plots of principal stress difference versus axial and radial strains. The specimen number, time to peak stress, and confining pressure at the start of the shear test are shown on each figure. Note that Specimen N06.2.27.0 was loaded to failure under a constant stress ratio of $\sigma_r/\sigma_a = 0.16$. Oil was found on Specimen N06.2.27.0 after the proportional loading test. However, it is believed that the leak occurred after application of the peak stress. The location of a hole found in the rubber membrane corresponded to the location of the shear plane in the specimen. As the specimen fractured under the loading, it is believed that the rough surface punctured the membrane. The data are nevertheless suspect. The data from that test indicated negligible hysteretic behavior during loading-unloading-reloading cycle performed prior to application of the peak stress. The average axial

strain at peak stress was approximately 1.4 percent. The average radial strain to peak stress was approximately 0.1 percent. The material continued to strain axially after peak stress, but did not show a large increase in radial strain. The results of the test on Specimen N06.2.31.0, shown in Figure 5.5, did not decrease in principal stress difference after peak; whereas the results of the other two tests on Specimens N06.2.26.7 and N06.2.27.0, shown in Figures 5.3 and 5.4, respectively, decreased slightly. The difference might have been caused by the difference in material. As previously noted, Specimen N06.2.31.0 was gray in color and had a higher unit weight than N06.2.26.7 and N06.2.27.0, which were red in color.

The shear test results are shown in Figure 5.6 as a plot of principal stress difference versus principal strain difference. The results indicate an average initial shear modulus G of 480×10^3 psi. The average principal strain difference at peak stress was approximately 1.6 percent, and, based on the limited data available, there appears to be no significant loading-rate effect on the stress-strain response of the U12n-06 tuff in shear.

Figure 5.7 presents plots of principal stress difference versus mean normal stress for all stages of the shear tests up to failure. The loading path to peak stress is shown as a dashed line, and the failure states are indicated by various symbols. The results indicate little or no effect of loading rate on the strength of the U12n-06 tuff. The peak strength of the gray material (Specimen N06.2.31.0) appears slightly higher than those of the red material (Specimens N06.2.26.7 and N06.2.27.0).

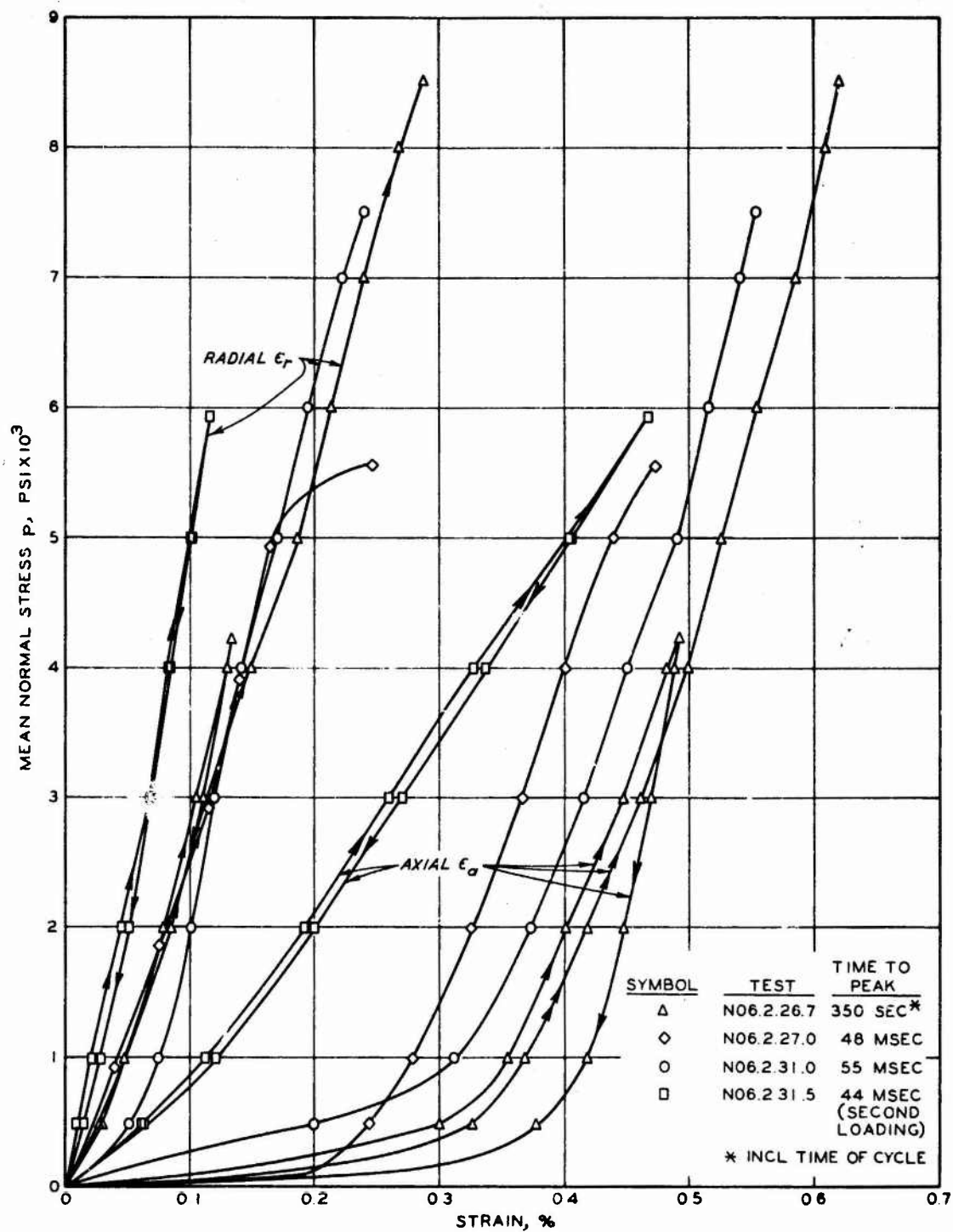


Figure 5.1 Stress-strain data from hydrostatic tests conducted on tuff from Tunnel U12n-06, Boring DE2.

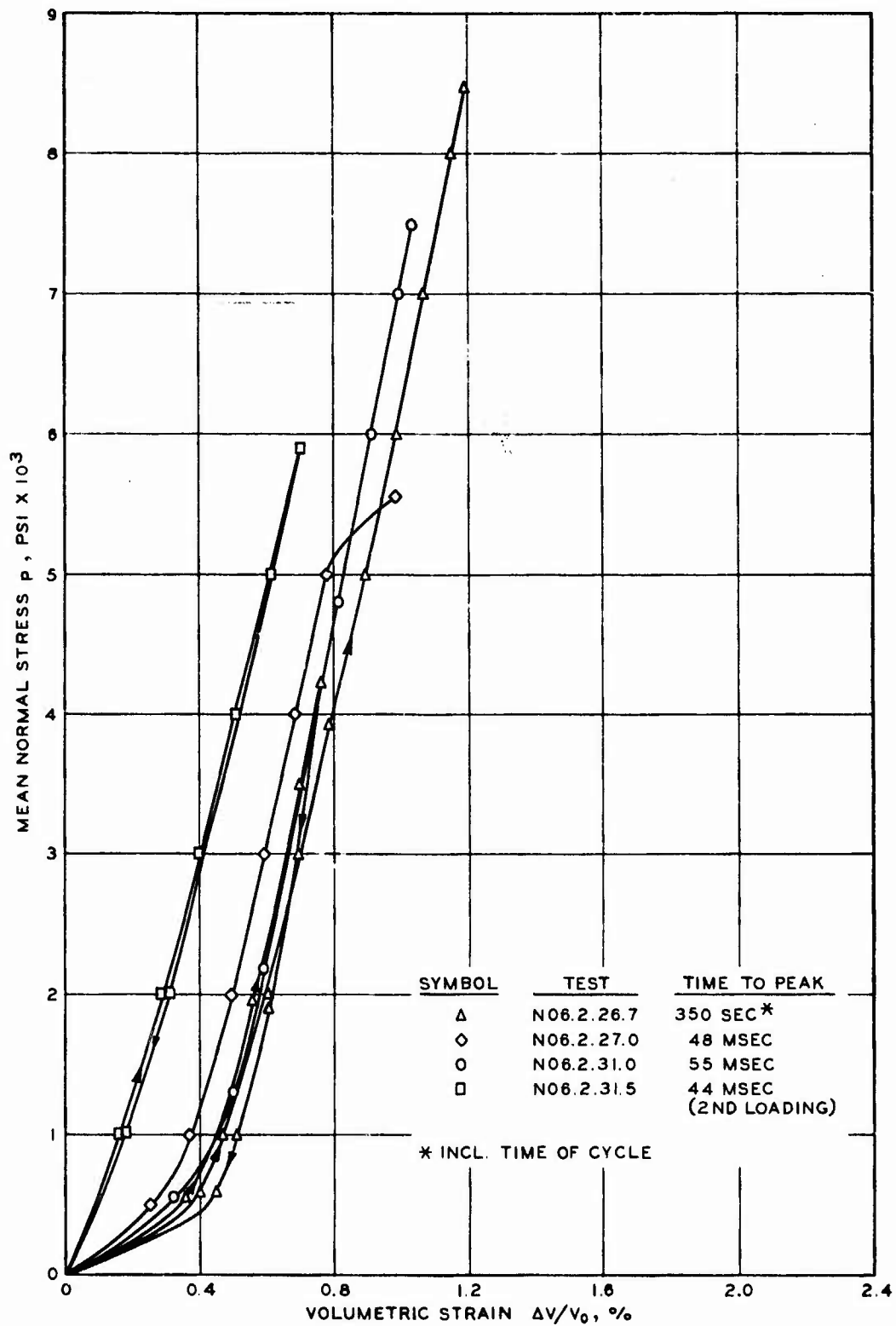


Figure 5.2 Stress versus volumetric strain showing the hydrostatic response of tuff from Tunnel U12n-06.

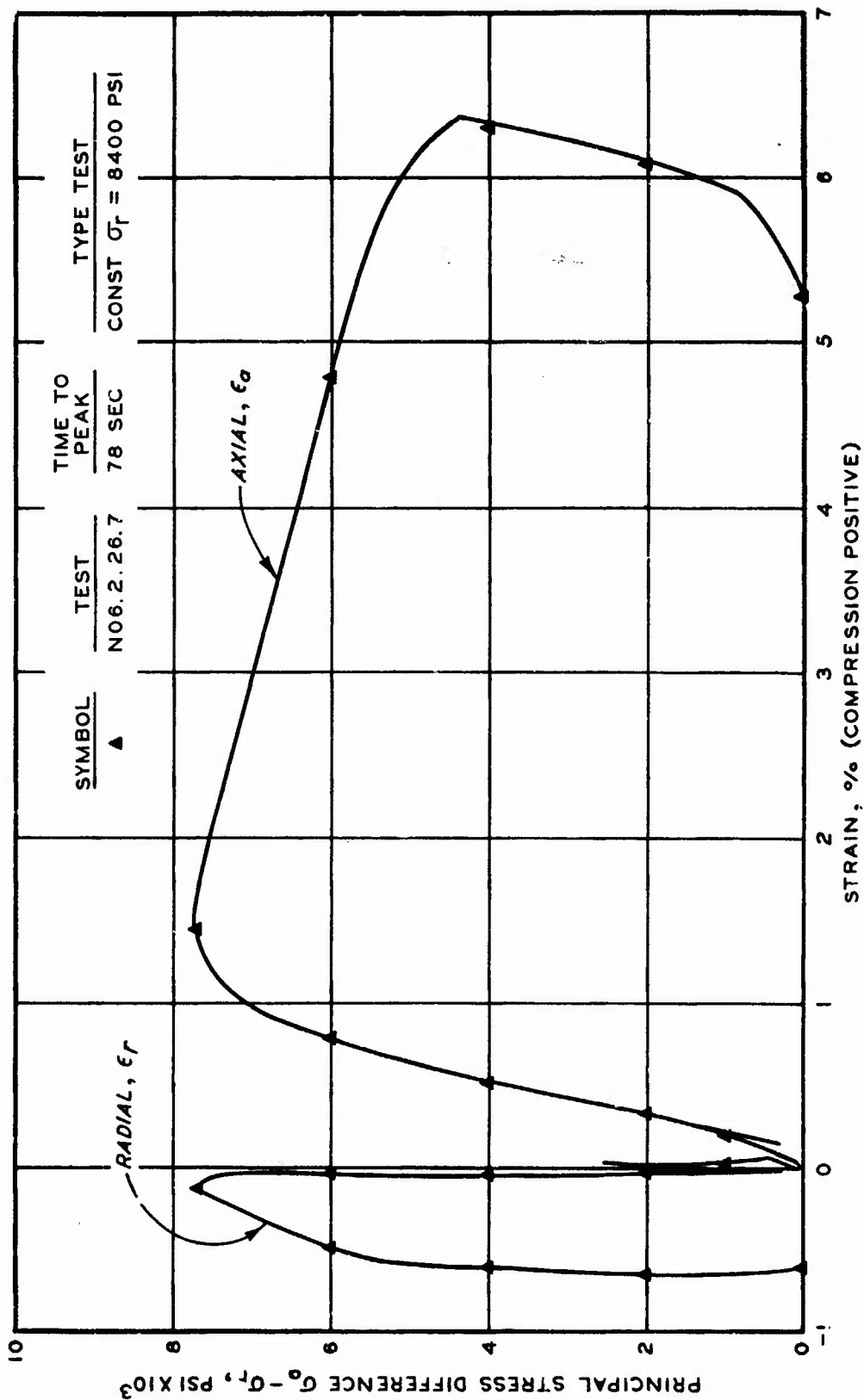


Figure 5.3 Shear test results from Test N06.2.26.7 showing axial and radial strain response.

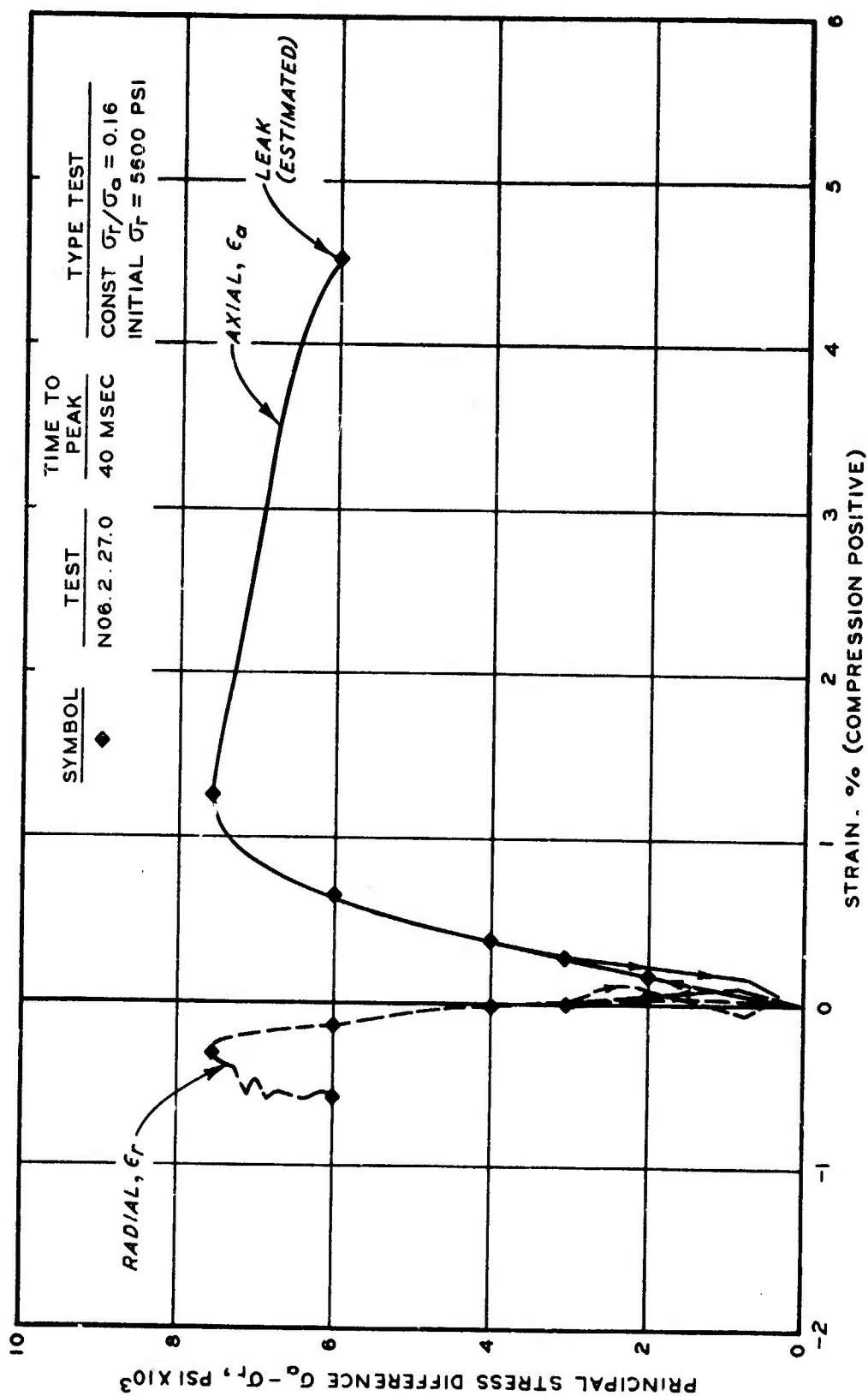


Figure 5.4 Shear test results from Test N06.2.27.0 showing axial and radial strain response.

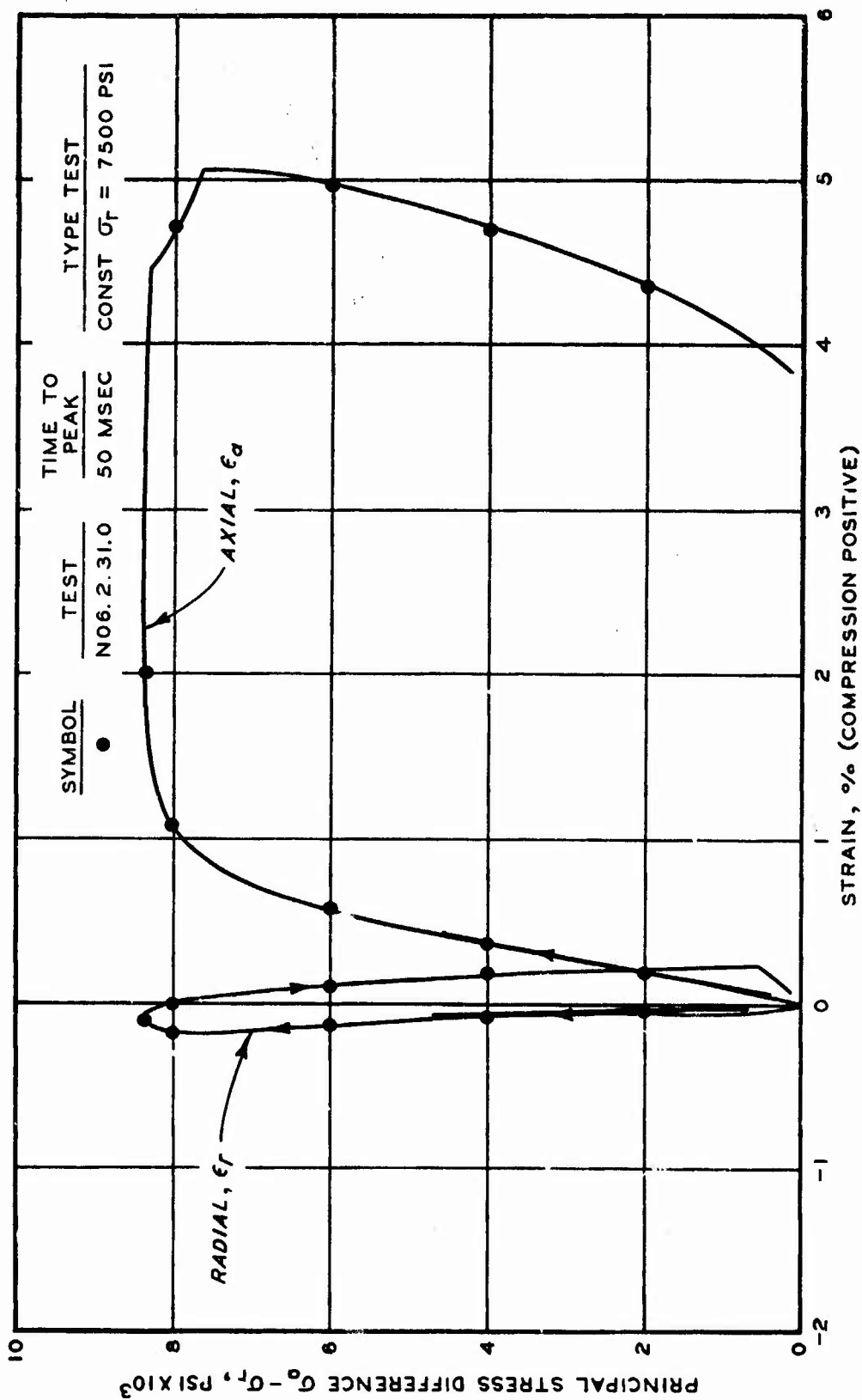


Figure 5.5 Shear test results from Test N06.2.31.0 showing axial and radial strain response.

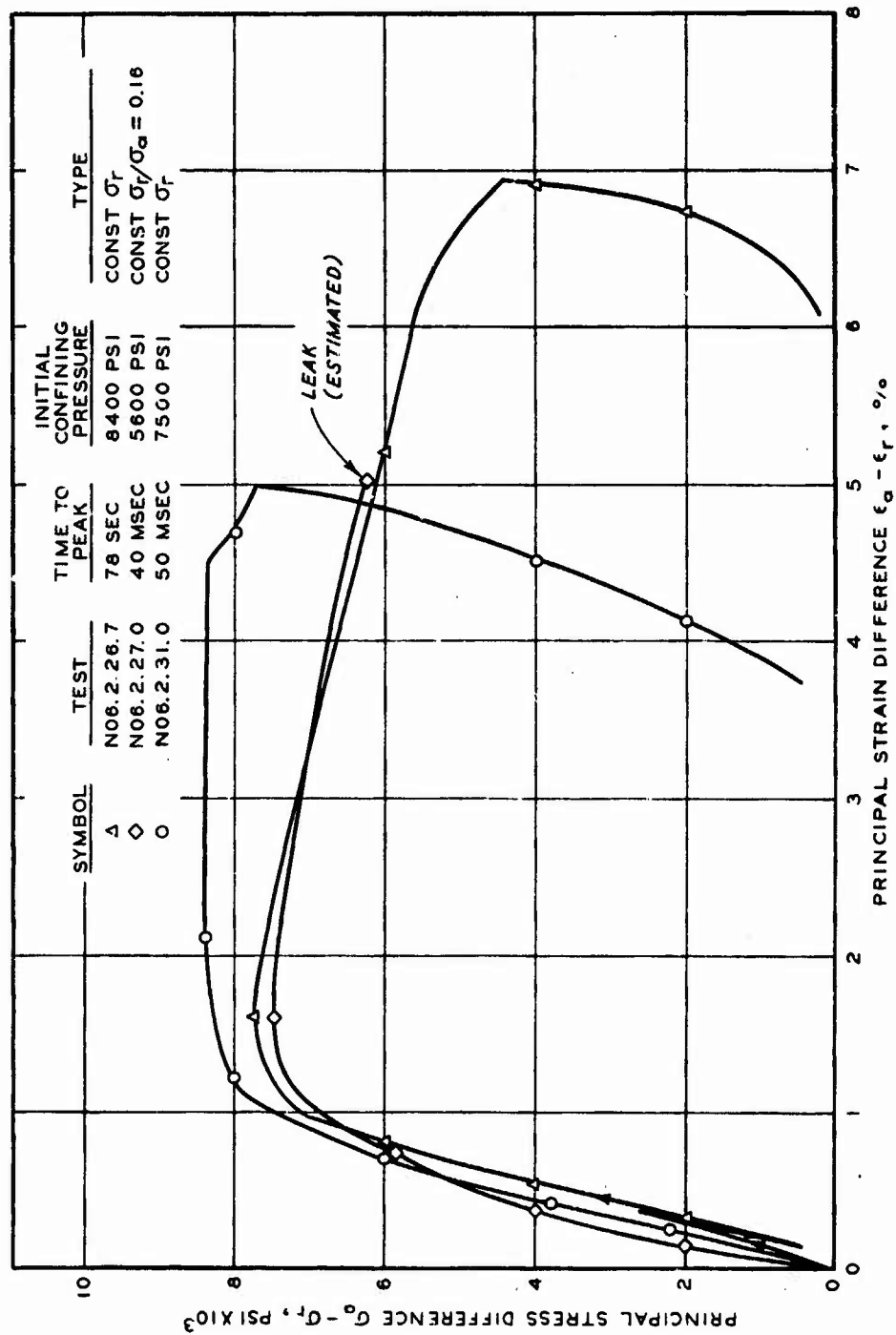


Figure 5.6 Principal stress difference versus principal strain difference showing results of shear tests on tuff from Tunnel U12n-06.

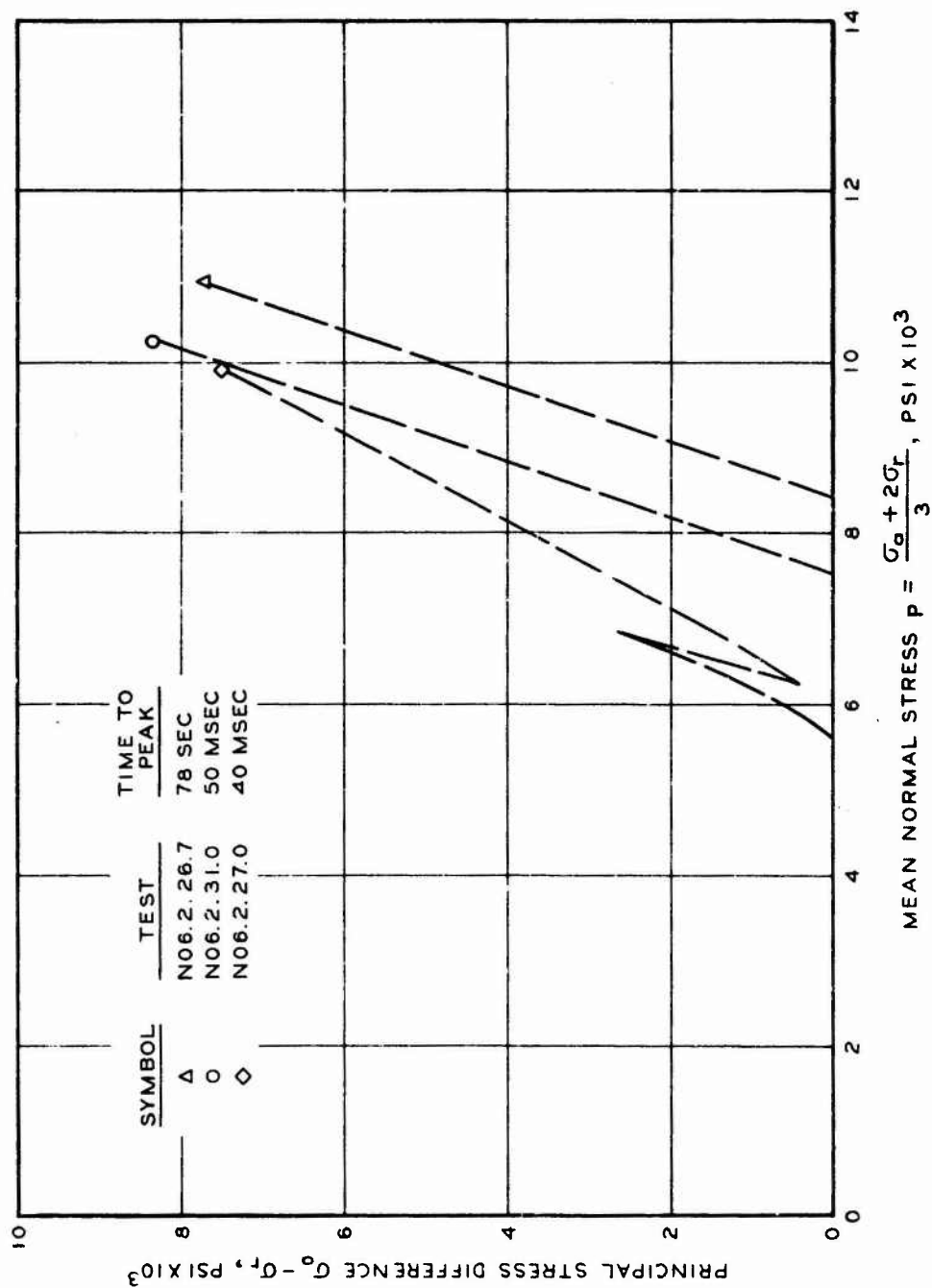


Figure 5.7 Principal stress difference versus mean normal stress showing peak stresses from shear tests on tuff from Tunnel U12n-06.

CHAPTER 6

COMPARISON OF THE TUFF MATERIALS

The experimental study was limited to a total of ten hydrostatic tests and eight shear tests on tuff materials from the two tunnels. All of the shear tests were conducted at confining pressures between 6,000 and 9,000 psi. The results indicate that there were actually four different tuff materials: two from each tunnel. For purposes of comparison, the two tuff materials from Tunnel U12n-06 will be combined because the differences noted were slight. The hydrostatic results on the two tuffs from Tunnel U12e-12 will not be combined because differences between those were significant, since the test data from each material appeared reasonably consistent for each loading condition. The data plots shown in this chapter are average curves drawn through the actual test data.

6.1 HYDROSTATIC RESPONSE

The average data for materials from the U12n-06 and U12e-12 tunnels are shown in Figure 6.1 as a plot of mean normal stress versus volumetric strain. The comparison indicates that the U12n-06 tuff and Boring 7B, U12e-12 tuff, show little difference in response characteristics. Both indicate a tangent bulk modulus of approximately 1.0×10^6 to 1.2×10^6 psi within the 1,000- to 8,000-psi pressure range. No significant effect of loading rate was noted on those types of tuff. The Site B (U12e-12) tuff, however, has a much lower bulk modulus (390×10^3 psi) over the same pressure range. The scatter prevented observations as to effect of loading rate on this material.

Differences were also noted in the individual strain responses during hydrostatic loading. All three types of tuff, i.e. the U12n-06 tuff and both U12e-12 tuffs, appeared to have the same axial strain response during loading. The radial strain responses of the U12n-06 and Boring DB7B (U12e-12) tuffs were approximately equal to the axial responses, indicating nearly isotropic behavior of those tuffs. The radial strain response of the Site B (U12e-12) tuff was two to three times that of

the axial response, indicating an anisotropic behavior.

6.2 SHEAR RESPONSE

A plot of principal stress difference versus principal strain difference for the materials from both tunnels is shown in Figure 6.2. Since differences between the U12e-12, Boring 7B and Site B, tuffs were not apparent, only one average curve based on the static test data is shown for U12e-12 material. The difference in initial shear modulus between the U12n-06 and U12e-12, Boring 7B, material is only approximately 10×10^3 psi. It should be noted, however, that the shear tests on the U12e-12 tuff did indicate some loading-rate effects on shear modulus, while those for the U12n-06 material did not. Therefore, the difference in shear modulus between the tuff under dynamic loading could be as great as 800×10^3 psi, based on the modulus of Specimen E.12.7B.8.0. The principal strain difference at peak stress was approximately 1.6 percent for the U12n-06 tuff and 2.5 percent for the U12e-12 tuff. Also, the U12n-06 tuff appeared to decrease in stress after the peak to a greater extent than did the U12e-12 material. The gray-colored U12n-06 tuff did not decrease in stress after the peak.

Figure 6.3 shows the failure points from all the shear tests in principal stress difference versus mean normal stress space. The U12n-06 tuff had an average strength of 7,800 psi at $p = 10-11 \times 10^3$ psi; significant loading-rate effects were not noted. The Boring 7B, U12e-12 tuff appeared to have a significant loading-rate effect and had a static strength of 6,000 psi and an average dynamic strength of 7,500 psi, both at $p = 11 \times 10^3$ psi. The Site B (U12e-12) tuff also indicated a loading-rate effect and static and dynamic strengths of 5,000 and 6,300 psi, respectively, were determined for the limited range of p .

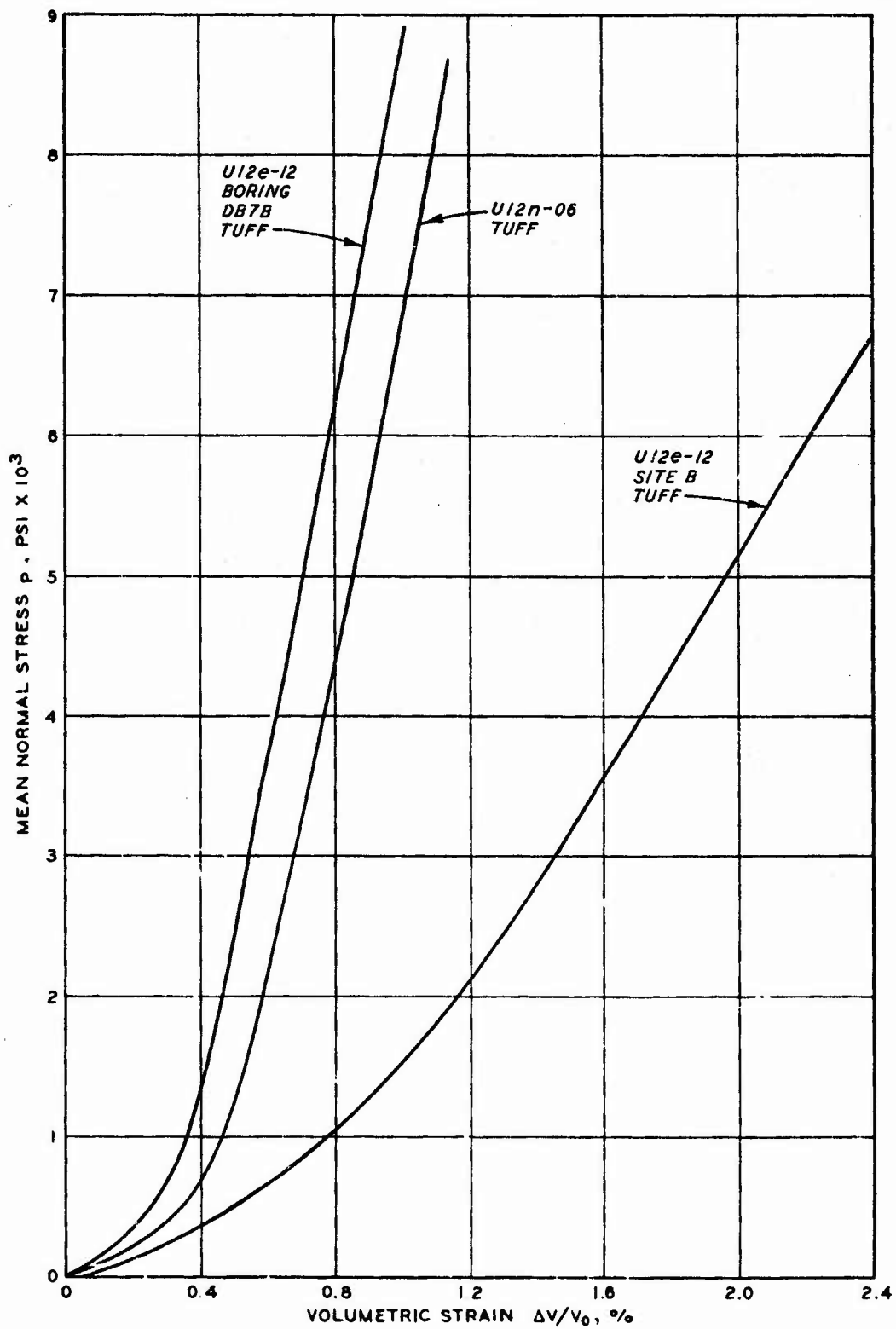


Figure 6.1 Stress versus volumetric strain showing the average hydrostatic responses for the tuff tested.

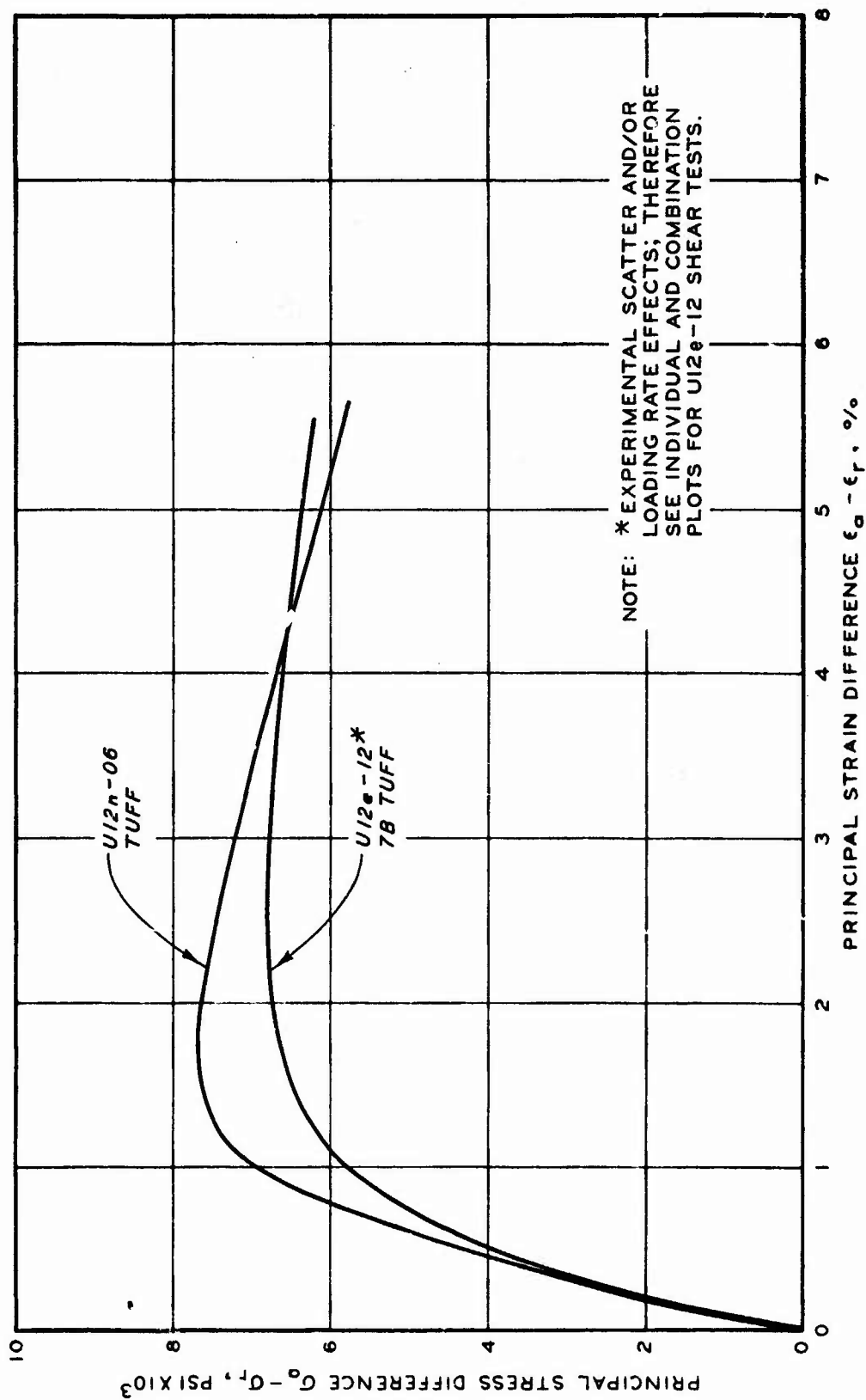


Figure 6.2 Principal stress difference versus principal strain difference showing average shear responses for the tuff tested.

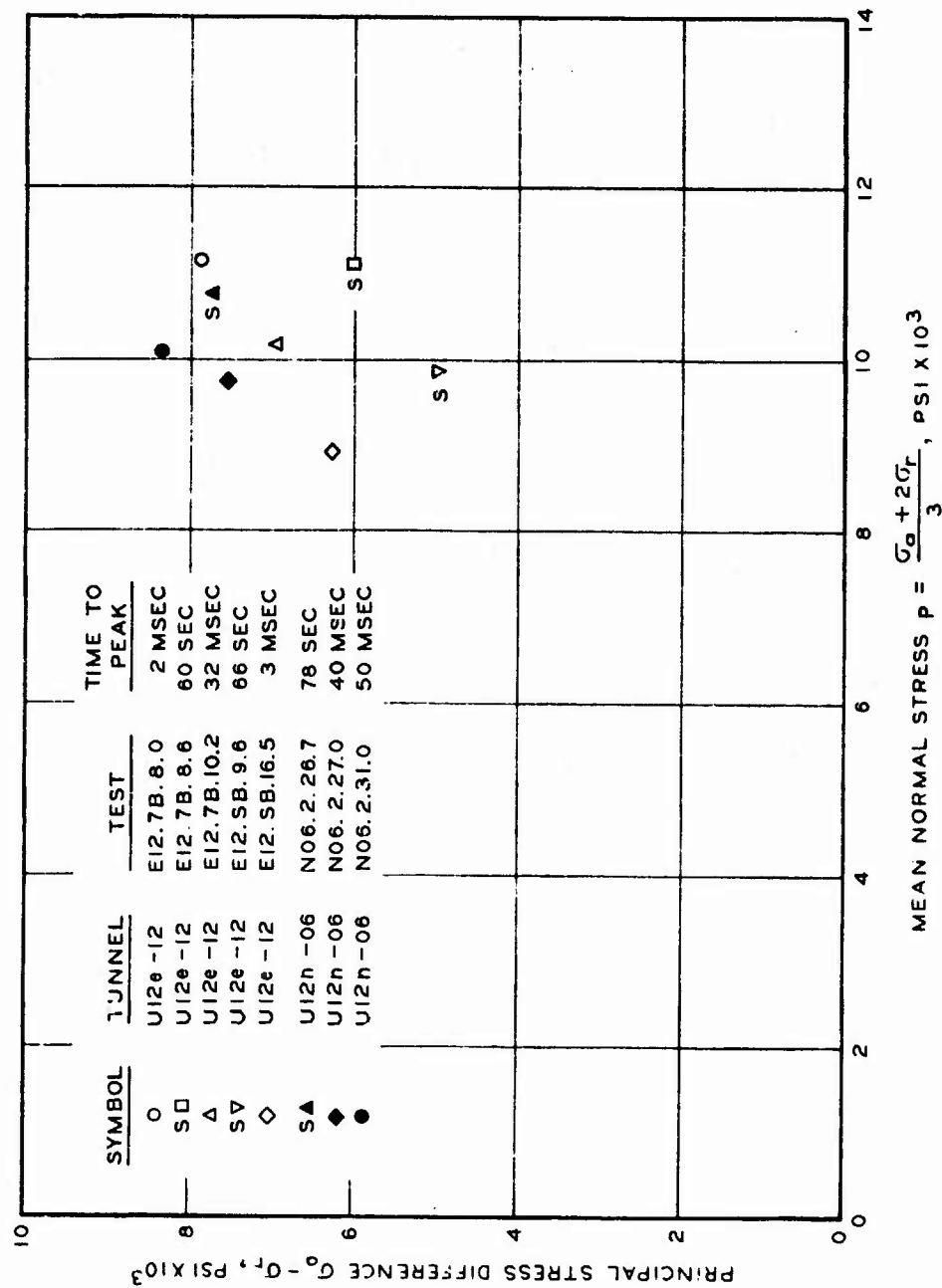


Figure 6.3 Principal stress difference versus mean normal stress showing the peak stress from the shear tests conducted on tuff from Tunnels U12e-12 and U12n-06.

CHAPTER 7

SUMMARY

The purpose of the study was to determine the dynamic response of tuff materials from two tunnels located at NTS and to note differences and similarities between the materials. A series of static and dynamic hydrostatic and shear tests to pressure levels of 8,000 psi were performed on NX-size tuff cores. A minimum of specimen preparation was performed by WES to prevent loss of water caused by air exposure.

7.1 U12e-12 TUFF

The Tunnel U12e-12 tuff received by WES included a nonfriable white-colored tuff and a friable, yellowish-colored tuff. Seven of the nine yellow-colored specimens were received in a fractured condition. The white tuff had a slightly higher average unit weight and lower water content than the yellow tuff. The hydrostatic response of the two materials differed; the yellow tuff indicated three times the volumetric strain as did the white tuff. The yellow tuff also was anisotropic in behavior. No loading-rate effect could be noted in the hydrostatic test. The shear tests indicated that the yellow tuff was slightly weaker than the white tuff. Loading-rate effects were noted; the dynamic to static peak stress ratio could be as high as 1.3.

7.2 U12n-06 TUFF

The Tunnel U12n-06 tuff received by WES included a gray-colored tuff and a red-colored tuff. The gray tuff had a higher unit weight and a lower water content than the red tuff. The hydrostatic and shear responses of the two tuffs were similar. No differences between the dynamic and static responses were noted.

7.3 DIFFERENCES NOTED BETWEEN TUFFS

The U12n-06 tuff had higher unit weights and lower water contents than did the U12e-12 tuff. The U12n-06 tuff and the white tuff from Tunnel U12e-12 had the same hydrostatic response characteristics and

both were nearly isotropic in hydrostatic loading. The yellow U12e-12 tuff was much softer. It had one-third the bulk modulus of the white tuff and was anisotropic in behavior. The largest difference observed in the response behavior of the tuffs during the shear loading was that the U12e-12 tuff exhibited greater radial strain after peak stress than the U12n-06 tuff. Also, the strength of the U12e-12 tuff was influenced by loading rate while that of the U12n-06 tuff was not. The Brazilian test tensile strength of the U12n-06 tuff was higher than the U12e-12 yellow tuff.